CENTER FOR
PORTLAND CEMENT CONCRETE
PAVEMENT TECHNOLOGY

Fly Ash Soil Stabilization for Non-Uniform Subgrade Soils, Volume II: Influence of Subgrade Non-Uniformity on PCC Pavement Performance

Final Report
April 2005

IOWA STATE UNIVERSITY

Sponsored by
the Iowa Highway Research Board (Project TR-461),
Federal Highway Administration (Project 4), and
Iowa Department of Transportation (CTRE Project 01-90)

Disclaimer Notice

The opinions, findings, and conclusions expressed in this publication are those of the authors and not necessarily those of the Iowa Department of Transportation, the Iowa Highway Research Board, and the Federal Highway Administration. The sponsors assume no liability for the contents or use of the information contained in this document. This report does not constitute a standard, specification, or regulation. The sponsors do not endorse products or manufacturers.

The contents of this report reflect the views of the authors, who are responsible for the facts and the accuracy of the information presented herein. This document is disseminated under the sponsorship of the U.S. Department of Transportation in the interest of information exchange. The U.S. Government assumes no liability for the contents or use of the information contained in this document. This report does not constitute a standard, specification, or regulation.

The U.S. Government does not endorse products or manufacturers. Trademarks or manufacturers' names appear in this report only because they are considered essential to the objective of the document.

About the PCC Center/CTRE

The Center for Portland Cement Concrete Pavement Technology (PCC Center) is housed at the Center for Transportation Research and Education (CTRE) at Iowa State University. The mission of the PCC Center is to advance the state of the art of portland cement concrete pavement technology. The center focuses on improving design, materials science, construction, and maintenance in order to produce a durable, cost-effective, sustainable pavement.

Technical Report Documentation Page

1. Report No. IHRB Project TR-461; FHWA Project 4	**2. Government Accession No.**	**3. Recipient's Catalog No.**
4. Title and Subtitle Fly Ash Soil Stabilization for Non-Uniform Subgrade Soils, Volume II: Influence of Subgrade Non-Uniformity on PCC Pavement Performance		**5. Report Date** April 2005 **6. Performing Organization Code** CTRE Project 01-90
7. Author(s) David J. White, Dale Harrington, Halil Ceylan, and Tyson Rupnow		**8. Performing Organization Report No.**
9. Performing Organization Name and Address Center for Transportation Research and Education Iowa State University 2901 South Loop Drive, Suite 3100 Ames, IA 50010-8634		**10. Work Unit No. (TRAIS)** **11. Contract or Grant No.**
12. Sponsoring Organization Names and Addresses Iowa Highway Research Board Iowa Department of Transportation 800 Lincoln Way Ames, IA 50010 Federal Highway Administration U.S. Department of Transportation 400 7th Street SW, HIPT-20 Washington, DC 20590		**13. Type of Report and Period Covered** Final Report **14. Sponsoring Agency Code**
15. Supplementary Notes Visit www.ctre.iastate.edu for color PDF files of this and other research reports.		

16. Abstract

To provide insight into subgrade non-uniformity and its effects on pavement performance, this study investigated the influence of non-uniform subgrade support on pavement responses (stress and deflection) that affect pavement performance.

Several reconstructed PCC pavement projects in Iowa were studied to document and evaluate the influence of subgrade/subbase non-uniformity on pavement performance. In situ field tests were performed at 12 sites to determine the subgrade/subbase engineering properties and develop a database of engineering parameter values for statistical and numerical analysis. Results of stiffness, moisture and density, strength, and soil classification were used to determine the spatial variability of a given property. Natural subgrade soils, fly ash-stabilized subgrade, reclaimed hydrated fly ash subbase, and granular subbase were studied. The influence of the spatial variability of subgrade/subbase on pavement performance was then evaluated by modeling the elastic properties of the pavement and subgrade using the ISLAB2000 finite element analysis program.

A major conclusion from this study is that non-uniform subgrade/subbase stiffness increases localized deflections and causes principal stress concentrations in the pavement, which can lead to fatigue cracking and other types of pavement distresses. Field data show that hydrated fly ash, self-cementing fly ash-stabilized subgrade, and granular subbases exhibit lower variability than natural subgrade soils. Pavement life should be increased through the use of more uniform subgrade support. Subgrade/subbase construction in the future should consider uniformity as a key to long-term pavement performance.

17. Key Words fly ash—long-term pavement performance—non-uniformity—stress and deflection responses—subgrade/subbase		**18. Distribution Statement** No restrictions.	
19. Security Classification (of this report) Unclassified.	**20. Security Classification (of this page)** Unclassified.	**21. No. of Pages** 46 plus appendix	**22. Price** NA

Form DOT F 1700.7 (8-72) **Reproduction of completed page authorized**

FLY ASH SOIL STABILIZATION FOR NON-UNIFORM SUBGRADE SOILS, VOLUME II

INFLUENCE OF SUBGRADE NON-UNIFORMITY ON PCC PAVEMENT PERFORMANCE

Final Report
April 2005

Principal Investigators
David J. White
Department of Civil and Construction Engineering, Iowa State University

Dale S. Harrington
Center for Transportation Research and Education, Iowa State University

Technical Contributor
Halil Ceylan
Department of Civil and Construction Engineering, Iowa State University

Research Assistant
Tyson Rupnow

Sponsored by
the Iowa Highway Research Board
(IHRB Project TR-461)

Preparation of this report was financed in part
through funds provided by the Iowa Department of Transportation
through its research management agreement with the
Center for Transportation Research and Education,
CTRE Project 01-90

A report from
Center for Transportation Research and Education
Iowa State University
2901 South Loop Drive, Suite 3100
Ames, IA 50010-8632
Phone: 515-294-8103
Fax: 515-294-0467
www.ctre.iastate.edu

TABLE OF CONTENTS

EXECUTIVE SUMMARY XI

INTRODUCTION 1

BACKGROUND 3

- Pavement Distress 3
- Spatial Variation of Soil Stiffness 3
- Support under PCC Pavements 4
- Case Study: Ohio SHRP Test Road, U.S. Rt. 23, Delaware, Ohio 4
- Subgrade Models for Numerical Analysis 5
  - Dense Liquid Model 5
  - Elastic Solid Model 6

METHODS 7

- Collection of Field Data 7
  - Task 1: Project Selection 7
  - Task 2: Grid Pavement and Document Pavement Quality 13
  - Task 3: DCP Testing 13
  - Task 4: Clegg Impact Hammer Testing 14
  - Task 5: GeoGauge Stiffness Testing 14
  - Task 6: Nuclear Density Gauge Testing 16
  - Task 7: Determine Subgrade/Subbase Index Properties 17
- Finite Element Modeling to Evaluate Pavement Response 17
  - Task 1: Estimate Modulus of Subgrade Reaction 18
  - Task 2: Select Pavement Engineering Properties and Loading Conditions 18
  - Task 4: Evaluate Pavement Responses 19
  - Task 5: Estimate Pavement Life from Numerical Analysis Output 20
- Statistical Analysis of Field and Numerical Results 20
  - Task 1: Determine the Mean, Standard Deviation, and COV Values for In-Situ Tests 20
  - Task 2: Perform SAS Analysis of ISLAB2000 Results 20

MATERIALS 21

- In Situ Test Results 21
  - Nuclear Density Gauge 21
  - GeoGauge Stiffness 21
  - Dynamic Cone Penetrometer 21
  - Clegg Impact Hammer 21
- Subgrade/Subbase Index Properties 21

RESULTS 27
Pavement Modeling 27
ISLAB2000 Results 27
Pavement Life Results 38
Statistical Analysis 39
Field Data Statistical Analysis 40

DISCUSSION 42
ISLAB2000 Pavement Modeling 42
Statistical Analysis 43
Field Data Statistical Analysis 43
ISLAB2000 Statistical Analysis 43

SUMMARY AND CONCLUSIONS 44

REFERENCES 46

APPENDIX – IN SITU TESTING RESULTS 47

LIST OF FIGURES

Figure 1. CBR data indicating non-uniform subgrade, US 61, Muscatine, IA 2
Figure 2. Project 1: Highway 63 in Eddyville, Iowa 8
Figure 3. Project 2: Highway 330 northeast of Bondurant, Iowa.....8
Figure 4. Location for projects 3 and 4: Knapp Street, Ames, Iowa.....10
Figure 5. Location for projects 5 and 6: I-235 West Des Moines, Iowa 10
Figure 6. Location for project 7: Highway 34 east of Fairfield, Iowa.....11
Figure 7. Location of project 8: U.S. Highway 218, Henry County 11
Figure 8. Location of project 9: Interstate 35 north of Highway 20.....12
Figure 9. Location for projects 10 and 11: Ames, Iowa.....12
Figure 10. Location for project 12: University and Guthrie Aves, Des Moines, Iowa 13
Figure 11. DCP testing on westbound entrance ramp of I-235 at 35th Street in West Des Moines, Iowa.....15
Figure 12. Clegg Impact Hammer.....15
Figure 13. GeoGauge 16
Figure 14. Nuclear Density Gauge.....16
Figure 15. Winkler spring foundation to simulate non-uniform subgrade/subbase stiffness 17

LIST OF TABLES

Table 1. In situ test grid spacing 14
Table 2. Input variables for ISLAB2000.....19
Table 3. Alternate axle design values 19
Table 4. Summary of nuclear density gauge data for all projects 22
Table 5. Summary of GeoGauge data for all projects.....23
Table 6. Summary of DCP index data for all projects 24
Table 7. Summary of CIVs for all projects 25
Table 8. USCS soil classifications for each project.....26
Table 9. Average maximum principal stresses and deflections for all projects using the in situ measured results for non-uniform subgrade/subbase stiffness.....37
Table 10. Average maximum principal stresss and deflections for all projects using idealized uniform subgrade 38
Table 11. Number of repetitions to failure for all projects using non-uniform and uniform subgrade support values using ISLAB2000 finite element solution results.....39

ACKNOWLEDGMENTS

This study was sponsored by the Iowa Highway Research Board (Project TR-461), the Federal Highway Administration (Cooperative Agreement DTFH61-01-X-00042, Project 4), the Iowa Fly Ash Affiliates, and the PCC Center Sponsored Research Fund. The support of these agencies is acknowledged and greatly appreciated.

EXECUTIVE SUMMARY

To provide insight into subgrade non-uniformity and its effects on pavement performance, the civil engineering and construction communities need to look at the whole pavement system to determine whether a more effective, economical solution exists for achieving long-term pavement performance. The purpose of this study was to investigate the influence of non-uniform subgrade support on critical pavement responses (maximum stresses, strains, and deflections) that affect pavement performance. This project set forth three objectives:

1. Generate field data from 10 to 12 local subgrade or pavement reconstruction projects in Iowa
2. Using the field data, develop numerical models to simulate pavement performance in terms of pavement stress and deflection responses
3. Conduct a statistical analysis of the results to determine whether a correlation exists between pavement life and subgrade non-uniformity

To achieve these objectives, several reconstructed Portland Cement Concrete (PCC) pavement projects in Iowa were studied to document and evaluate the influence of subgrade/subbase non-uniformity on pavement performance. In situ field tests were performed at 12 sites to determine the subgrade/subbase engineering properties and develop a database of engineering parameter values for statistical and numerical analysis. Field tests included the following: Dynamic Cone Penetrometer, nuclear density gauge, GeoGauge stiffness, and Clegg Impact Hammer tests. Tests were performed in a grid pattern (approximately 2.5 m x 2.5 m over an area about 7.5 m wide by 30 m long) to develop a spatial database of the subgrade/subbase engineering property values. Results of stiffness, moisture and density, strength, and soil classification were then used to determine the spatial variability of a given property. Natural subgrade soils, fly ash-stabilized subgrade, reclaimed hydrated fly ash subbase, and granular subbase were studied. The influence of the spatial variability of subgrade/subbase on pavement performance was then evaluated by modeling the elastic properties of the pavement structure and the pavement foundation using the ISLAB2000 finite element model. Results show that non-uniform subgrade/subbase support increases localized deflections and causes stress concentrations in the pavement, which can lead to premature failures, fatigue cracking, faulting, pumping, rutting, and other types of pavement distresses for rigid and flexible pavement systems.

Field data show that hydrated fly ash (HFA), self-cementing fly ash-stabilized subgrade, and granular subbases exhibit lower variability than natural subgrade soils. This was determined by calculating and comparing the coefficient of variation (COV) for the stiffness of natural subgrade (COV up to 71 percent), fly ash-stabilized subgrade (COV about 22 percent), reclaimed HFA (COV about 20 percent), and granular subbase (COV about 16 percent). Results from analytical pavement modeling using the ISLAB2000 finite element program show that when pavement foundations are modeled using a uniform subgrade, the maximum principal stresses and deflections are reduced in the pavement structure and thus the fatigue life increases. A major conclusion from this study is that pavement performance is adversely affected by non-uniform pavement foundations. Pavement life can be increased and pavement performance improved through using more uniform subgrade/subbase support. Pavement subgrade/subbase construction in the future should consider uniformity as one of the key issues for long-term pavement performance.

INTRODUCTION

Portland cement concrete (PCC) pavement reconstruction projects were studied in Iowa to better understand the influence of subgrade/subbase non-uniformity (i.e., stiffness and volumetric stability) on long-term pavement performance. Some recognized direct causes of subgrade/subbase non-uniformity include (1) expansive soils; (2) differential frost heave and subgrade softening; (3) non-uniform strength and stiffness due to variable soil type, moisture content, and density; (4) pumping and rutting; (5) cut/fill transitions; and (6) poor grading. Some techniques to overcome these subgrade deficiencies include the following:

- Moisture-density control during construction
- Proper soil identification and placement
- Overexcavation and replacement with select materials
- Mechanical and chemical soil stabilization
- On-site soil mixing to produce well-graded composite materials
- Good grading techniques (e.g., uniform compaction energy/lift thickness)
- Waterproofing of the subgrade and control of moisture fluctuations

Although emphasis is placed on subgrade/subbase stiffness (i.e., modulus of subgrade reaction, k_s) for designing PCC pavement thickness, performance monitoring suggests that uniformity of stiffness is the key for ensuring long-term performance (American Concrete Pavement Association 2001). Because of the relatively high flexural stiffness of PCC pavements, the subgrade does not necessarily require high strength, but, importantly, the subgrade/subbase should be uniform, with no abrupt changes in "degree of support" (American Concrete Pavement Association 1995). Yoder (1959) also indicates that the uniformity has a significant influence on the "stress intensity" and "deflection" of the pavement layer and that the magnitude of stresses in the upper pavement layer depends on a combination of traffic loads and "uniformity of subgrade support."

Non-uniform stiffness and the resulting stress intensity contribute to fatigue cracking and differential settlement (deflection) in the pavement layer and eventually to an uneven pavement surface. This uneven surface causes a rough ride for traffic and contributes to early pavement deterioration and high maintenance costs.

Figure 1 shows field data for a 300 m–long test section in Iowa. California Bearing Ratio (CBR) data, correlated from Dynamic Cone Penetrometer (DCP) tests, show that the subgrade is severely non-uniform, which at this site is believed to be a result of variable soil type and poor moisture and density control during subgrade construction.

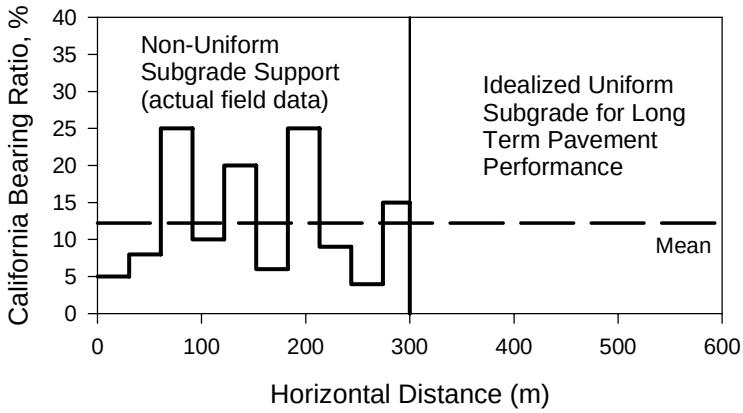

Figure 1. CBR data indicating non-uniform subgrade, US 61, Muscatine, IA

This project was undertaken to investigate further the influence of non-uniform subgrade/subbase support on pavement stresses and deflections that directly impact pavement performance. The three objectives needed to accomplish this goal were as follows:

1. Generate field data from 10 to 12 local subgrade or pavement reconstruction projects in Iowa
2. Using field data, develop numerical models to simulate pavement performance in terms of pavement stress and deflection responses
3. Conduct statistical analysis of the results to determine whether a correlation exists between pavement life and subgrade non-uniformity

Conclusions of the research confirmed that there is a link between pavement performance and subgrade non-uniformity. Analytical modeling of pavement systems indicate that a uniform subgrade system reduces critical pavement responses (maximum stresses, strains, and deflections) that lead to increased pavement life. Statistical analysis, using mean and coefficient of variation (COV) values, shows that field results for hydrated fly ash (HFA), granular subbase, and self-cementing fly ash-treated subgrade tend to be more uniform and have higher stiffness than Iowa soil subgrades. Analysis of the finite element results further shows that a uniform pavement foundation system produces stresses and deflections, with less variability.

BACKGROUND

Since the first concrete pavement was placed in Bellefontaine, Ohio in 1893, rigid pavement design and analysis have become increasingly more important. In 2001 there were approximately 59,000 miles of rigid pavement in the United States (Huang 2004). With pavement rehabilitation projects and costs continuously rising, research must investigate the influence of subgrade non-uniformity and its effects on pavement performance.

To provide context for this study, this background section briefly introduces sources of pavement stress, pavement failure mechanisms, and some basic subgrade numerical model approaches used in this investigation. This review also briefly describes past research that documents the effects of spatial variation.

Pavement Distress

PCC pavement distresses come from two sources: design and construction deficiency (Huang 2004). Distresses can be classified further into functional, structural, load associated, and non-load associated distresses. Types of distress in PCC pavements include blowups, corner breaks, durability cracking, joint faulting, joint deterioration, longitudinal cracks, popouts, pumping and water bleeding, spalling, transverse cracks, edge punchout, and localized distress (Strategic Highway Research Program [SHRP] 1990).

Several of these distresses, such as blowups, durability cracking, and popouts, are beyond the designer's control because they are mainly non-load associated distresses. These distresses are effectively controlled with proper inspection and construction practices. The rest of this section will focus on load associated distresses, specifically faulting and joint deterioration.

SHRP (1990) and Huang (2004) describe faulting as a difference in elevation across a transverse or longitudinal joint. Faulting is caused by either a buildup of loose material under the trailing slab or depression of the leading slab (Huang 2004). The buildup or erosion of materials is caused by pumping and water bleeding. Pumping is the ejection of water and solids from a crack under heavy loads (Bhatti *et al.* 1996). This action is detrimental to pavement performance, causing subgrade non-uniformity. Bhatti *et al.* (1996) note that in order to prevent pumping and the associated loss of support, a drainable base needs to be installed.

Maximum pavement stresses are usually on the center edge of a fully supported slab (Huang 2004). When pumping causes erosion and loss of support at a joint, however, the maximum stress occurs at the joint for a corner loading case (Huang 2004). Loss of support can significantly increase pavement stresses, thus increasing pavement distresses and ultimately leading to premature failure of the pavement section.

Spatial Variation of Soil Stiffness

Soil parameters vary from point to point, even in normally homogeneous layers. Grabe (1993) shows that it is necessary to describe the spatial variation in order to predict geotechnical

performance and deal with risk and reliability. Differential stiffness values lead to differential settlements. These differential settlements then cause dynamic forces that induce further settlement.

Key conclusions from this study include the following: (1) measurements show that there is no pattern of measured soil stiffness, (2) natural variation of the subgrade is transmitted to the pavement due to repeated loadings of passing vehicles, and (3) soil transmits its variance gradually to the surface of the pavement (Grabe 1993).

Support under PCC Pavements

Stresses and deflection affect the performance of a PCC slab and depend on several support factors, including the following:

- Subgrade soil stiffness
- Base type, stiffness, and thickness
- Frictional resistance between the slab and the base
- Freeze-thaw action in the base and subgrade
- Seasonal moisture levels in the subgrade and untreated base
- Load transfer at the joints
- Erosion of base or subgrade material from traffic loading, poor drainage, or pavement movement
- Temperature and moisture gradients within the slab. (Darter *et al*. 1995)

Research suggests that design k-values should be top of embankment because top of base k-values are unreasonably high and are not recommended for design. Research also recommends that the design k-value be a seasonally adjusted k-value and account for some loss of support due to erosion. Further, an increased k-value will always reduce tensile stress in the slab due to loading if there is no temperature gradient, and k-values increase for shorter spacing, thereby increasing the number of applications to terminal serviceability (Darter et al. 1995).

Case Study: Ohio SHRP Test Road, U.S. Rt. 23, Delaware, Ohio

This project was constructed in August 1996 to study four objectives: (1) structural factors for flexible pavements, (2) structural factors for rigid pavements, (3) environmental effects in the absence of heavy traffic, and (4) asphalt program field verification. For the purposes of this report, objectives (1) through (3) are discussed.

For this study, the project length was 3 miles, the northbound lanes were constructed of PCC, and the southbound lanes were constructed of asphalt concrete (AC). The ramps to the southbound section were constructed of PCC and AC to investigate environmental effects. Site topography was flat and fine grained soils, A-4, A-6, and A-7-6, were present with a depth to groundwater of about 4.3 feet below the surface. Several base types and combinations were used for this project, including dense-graded aggregate base, asphalt-treated base, permeable asphalt-treated base, permeable cement-treated base, and a lean concrete base.

Subgrade soils were compacted by sheepsfoot roller to 100% maximum dry density to 12 inches below pavement subgrade surface. Field tests included nuclear density gauge and falling weight deflectometer (FWD) on the subgrade, base, and pavement after the completion of each layer. The FWD data was used to back-calculate elastic modulus values.

Conclusions from this study show great variability in subgrade stiffness as calculated from the FWD data, even though all subgrade soil layers satisfied compaction requirements. Excessive rutting was observed in one asphalt section and it was determined that insufficient subgrade stiffness led to premature pavement distress. This observation reinforced the conclusion that relative compaction alone is not enough to ensure pavement performance and that subgrade soil stiffness must be measured and controlled (Sargand *et al.* 2000).

Subgrade Models for Numerical Analysis

In geotechnical engineering, the solution of a slab-on-grade soil-structure interaction problem has been simplified. Concrete pavements and foundations are generally treated as an elastic plate and the soil supporting the pavement or foundation is assumed to be linear, elastic, isotropic, and homogeneous. In reality, the stress-strain behavior of the soil is nonlinear, irreversible, anisotropic, and inhomogeneous.

The above mentioned soil complexities have led to the development of idealized models to provide a representation of soil behavior under certain loading and boundary conditions. There are two widely accepted subgrade models: dense liquid and elastic solid (Huang 2004; Khazanovich 1994; Ioannides 1984; Darter *et al.* 1995). Authors are quick to note that although the dense liquid and elastic solid models are widely used to simplify the slab-on-grade soil-structure interaction, real soil behavior actually falls somewhere between the two models.

The first section addressing subgrade models will discuss the dense liquid model's advantages and disadvantages. The second section addressing subgrade models will discuss the elastic solid model's advantages and disadvantages.

Dense Liquid Model

The dense liquid model assumes that the supporting soil acts like a bed of closely spaced, independent, linear springs (Khazanovich 1994; Ioannides 1984; Darter *et al.* 1995). Westergaard simplified the model by stating that the reactive pressure between the slab and the subgrade at any given point is directly proportional to the deflection at that point and is independent of the deflections at other points (Huang 2004; Ioannides 1984; Darter et al. 1995; Khazanovich 1994). This type of foundation is also called a Winkler foundation or a Winkler spring.

Westergaard is credited for the studies of pavement stresses and deflections using the dense liquid foundation. Westergaard developed equations for temperature curling and three loading cases for large slabs, including corner loading, edge loading, and interior loading (Huang 2004). This approach assumes that full contact exists between the slab and subgrade.

An advantage of the dense liquid model is that it allows consideration of the load transfer at PCC slab joints. This is especially useful because it allows the development of a few major distress types, including faulting, pumping, and corner breaking (Khazanovich 1994).

As Khazanovich (1994) notes, a disadvantage of the dense liquid model is that it assumes no shear interaction between adjacent spring elements, resulting in a foundation parameter, k, that is sensitive to the radius of the plate used to determine the parameter (Darter *et al.* 1995). The foundation parameter, k, is determined by dividing the change in stress by the change in deflection (Bowles 1996). Bowles (1996) noted that the plate load test required to obtain k is an expensive, time consuming test requiring large loads to produce small deflections.

Huang (2004) provides several k value approximations for soils as follows: low support k values range from 75-120 pci, medium support k values range from 130-170 pci, high support k values range from 180-220 pci, and very high support k values range from 250-400 pci. Soils characterized by low support are fine grained soils with high silt and clay contents, soils providing medium support are sand and gravel mixtures with moderate clay or silt contents, and soils exhibiting high support are sand and gravel mixtures free of plastic fines. Cement-treated subbases exhibit very high support (Huang 2004).

Elastic Solid Model

The elastic solid model is considered a linearly elastic, isotropic, homogeneous solid of semi-infinite extent (Ioannides 1984). Darter *et al*. (1995) state that under the elastic solid model, the load applied to the surface of the foundation is assumed to produce a continuous and infinite deflection basin.

Ioannides (1984) and Khazanovich (1994) note that one benefit of the elastic solid foundation is that it is a sufficiently realistic representation of actual subgrade behavior because it takes into account the effect of shear interaction between adjacent support elements. This effect leads to deflections influenced by stresses adjacent to the point at which the deflection is being measured.

Disadvantages of the elastic solid foundation model include its mathematical complexity and its inability to model the discontinuity of a deflection profile that occurs at the joints (Ioannides 1984; Khazanovich 1994).

METHODS

The methods section overviews the in situ testing, numerical modeling, and statistical methods used throughout this study. Methods include (1) collection of field data, (2) finite element modeling to evaluate pavement response, and (3) statistical analysis of field and numerical results. Several tasks defined during this phase of the project are described under various project objectives.

Collection of Field Data

Field data were generated to provide technical data for generating subgrade finite element models to evaluate pavement performance. Field data were generated using a grid system and by conducting several in situ tests at each grid point.

Task 1: Project Selection

Project selection began in late July 2002. Research of existing pavement removal projects was conducted using Iowa Department of Transportation (Iowa DOT) personnel input. In this task, twelve project locations were identified and tested. Subgrade/subbase materials included representative Iowa soils as well as HFA and Iowa DOT-specified granular subbases (special backfill and modified subbase). The following summarizes the project locations and test dates. In each map, a circle indicates the project location and the north direction is oriented upward.

<u>Project 1</u>

This project is located along Highway 63 in Eddyville, Iowa. This project utilized HFA from the nearby Ottumwa Generating Station as a subbase material. The HFA was chosen in lieu of select subgrade soils on the project due to the limited availability of select soils. The project length (about one mile) was constructed and tested in August 2002. Figure 2 shows the map location of Project 1.

<u>Project 2</u>

This project is located along Highway 330 about five miles northeast of Bondurant, Iowa. At this site, a section of Highway 330 had been abandoned after pavement removal. This pavement had been constructed directly on the subgrade soil. Subgrade soils were tested and documented immediately after pavement removal in September 2002. Figure 3 shows the project location.

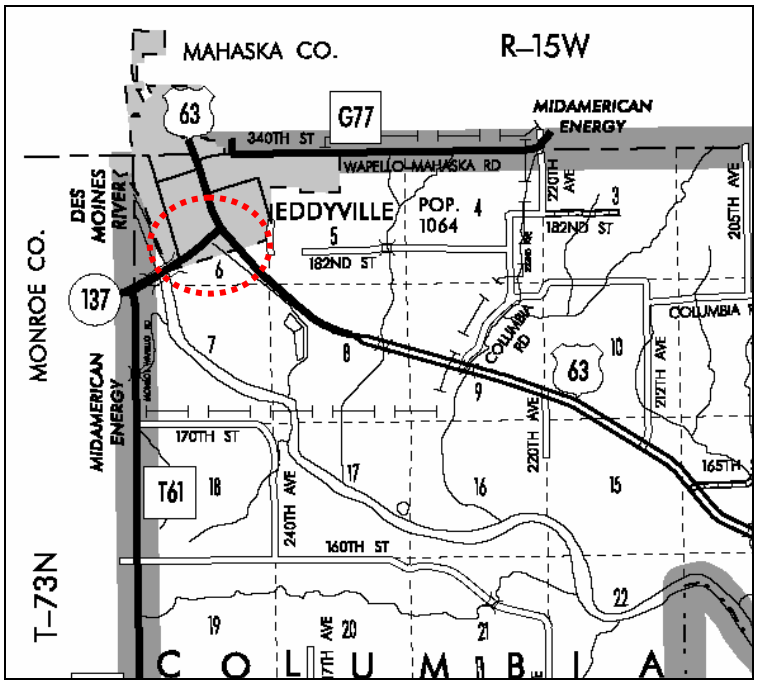

Figure 2. Project 1: Highway 63 in Eddyville, Iowa

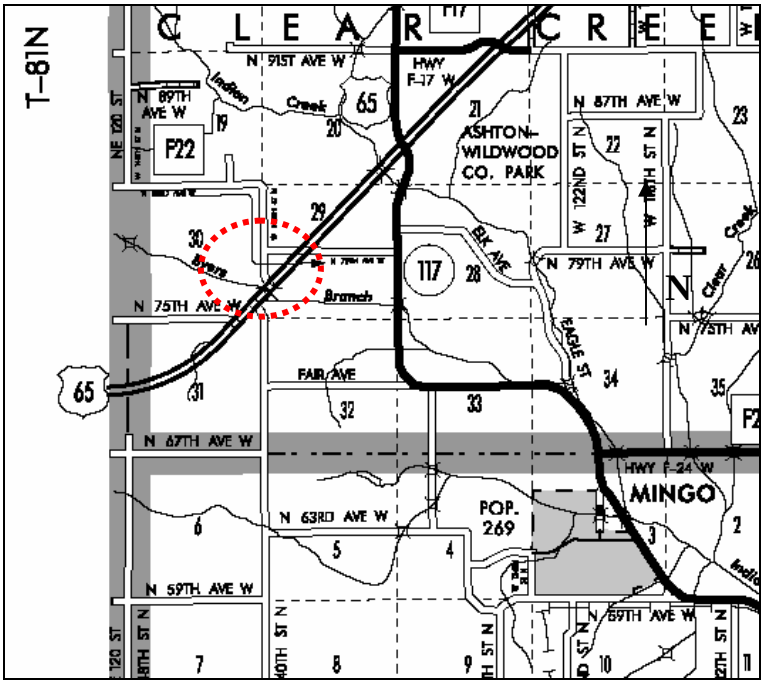

Figure 3. Project 2: Highway 330 northeast of Bondurant, Iowa

Projects 3 and 4

Project 3 is located in Ames, Iowa on a deteriorated section of Knapp Street. Knapp Street is located two blocks south of Lincoln Way, just west of the Iowa State University campus. The project reconstruction was about a half-mile in length. Subgrade soils were documented, tested, and modeled. Testing was carried out in May 2003. Project 4 is also on Knapp Street in Ames, Iowa. Documentation and testing of the newly placed granular subbase was completed in June 2003. Figure 4 shows the location of projects 3 and 4.

Projects 5 and 6

Project 5 is located in West Des Moines, Iowa along the Interstate 235 corridor at 35th Street. At this site, the subgrade supporting the existing westbound I-235 entrance ramp was tested after pavement removal. Testing was completed in May 2003. Project 6 is also located in West Des Moines, but on the newly constructed westbound I-235 entrance ramp at 35th Street. Tests were performed on the modified subbase in June 2003. Figure 5 shows the location of projects 5 and 6.

Project 7

This project is located on state Highway 34 about five miles east of Fairfield, Iowa. Testing at this site was performed in July 2003 on subgrade embankment soils previously constructed during the 2002 construction season. Figure 6 shows the project location.

Project 8

This project is located on U.S. Highway 218 in Henry County about three miles north of the border between Henry County and Lee County. Field tests were performed July 2003 on a newly constructed embankment section built earlier in the construction season. Figure 7 shows the project location.

Project 9

This project involved testing subgrade soils on northbound Interstate 35 about two miles north of U.S. Highway 20. Testing was conducted after the existing pavement was removed in June 2003. Figure 8 shows the project location.

Projects 10 and 11

Project 10 stemmed from research on subgrade improvement carried out in Ames, Iowa at the Jack Trice Stadium drive and parking area, located on Elwood Drive about one mile north of U.S. Highway 30. Testing took place in September 2002 on a deteriorated asphalt pavement subgrade. Project 11 is also at Jack Trice Stadium, but was carried out after self-cementing fly ash subgrade stabilization had been completed. Testing was completed in September 2002 before the asphalt surface layer was placed. Figure 9 shows the locations of projects 10 and 11.

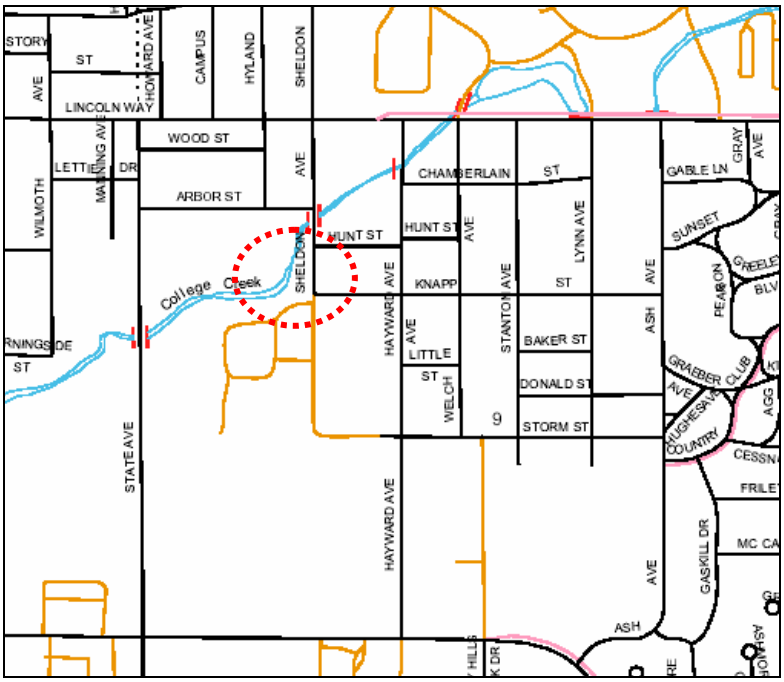

Figure 4. Location for projects 3 and 4: Knapp Street, Ames, Iowa

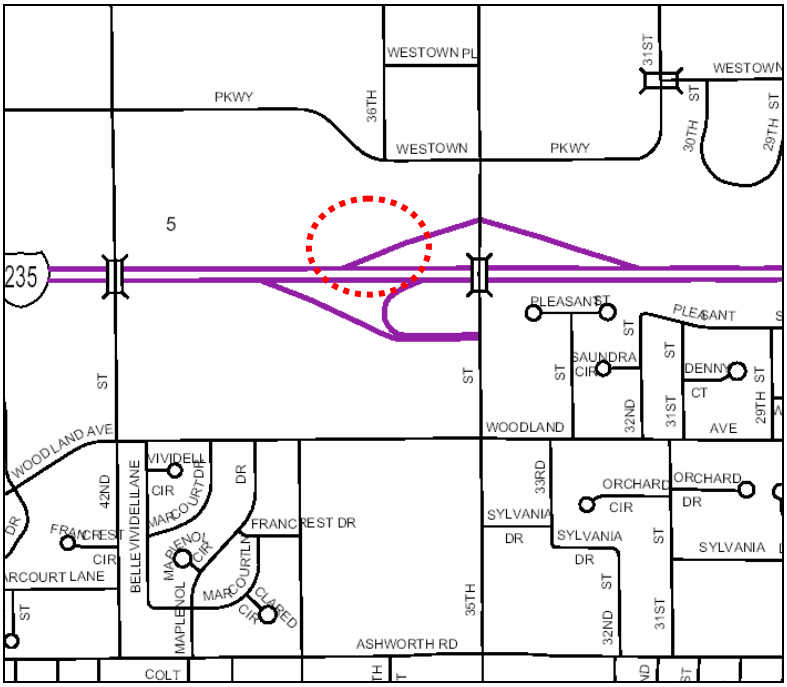

Figure 5. Location for projects 5 and 6: I-235 West Des Moines, Iowa

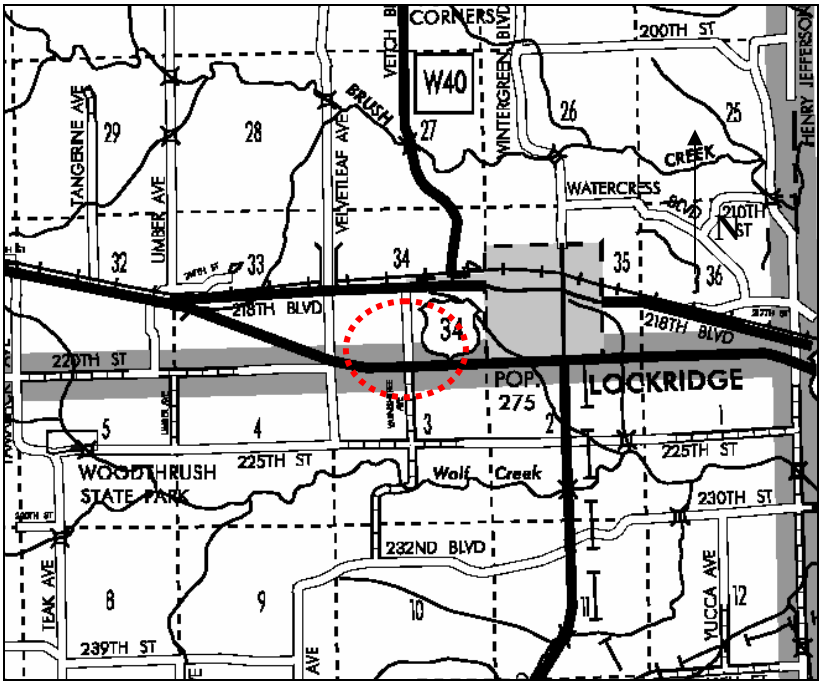

Figure 6. Location for project 7: Highway 34 east of Fairfield, Iowa

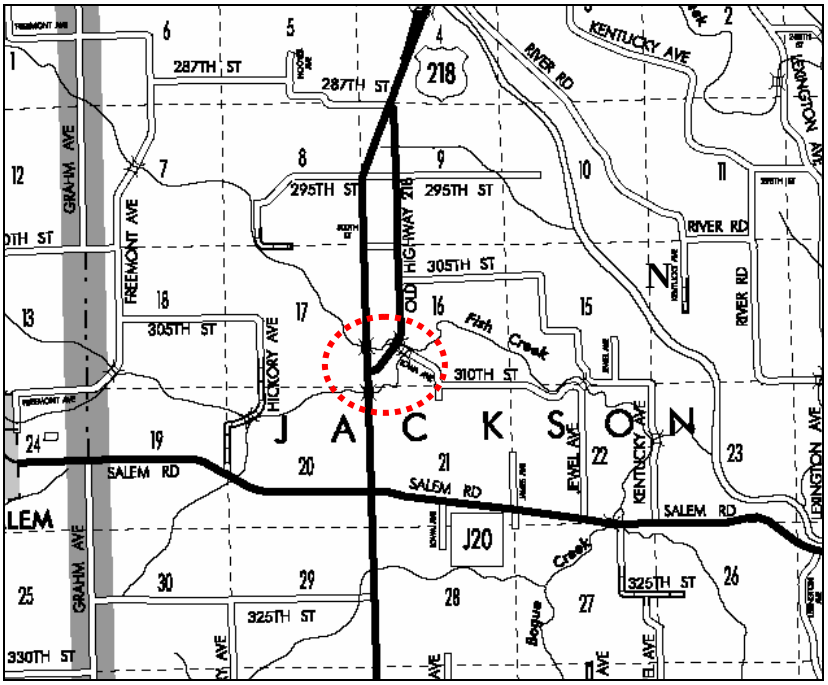

Figure 7. Location of project 8: U.S. Highway 218, Henry County

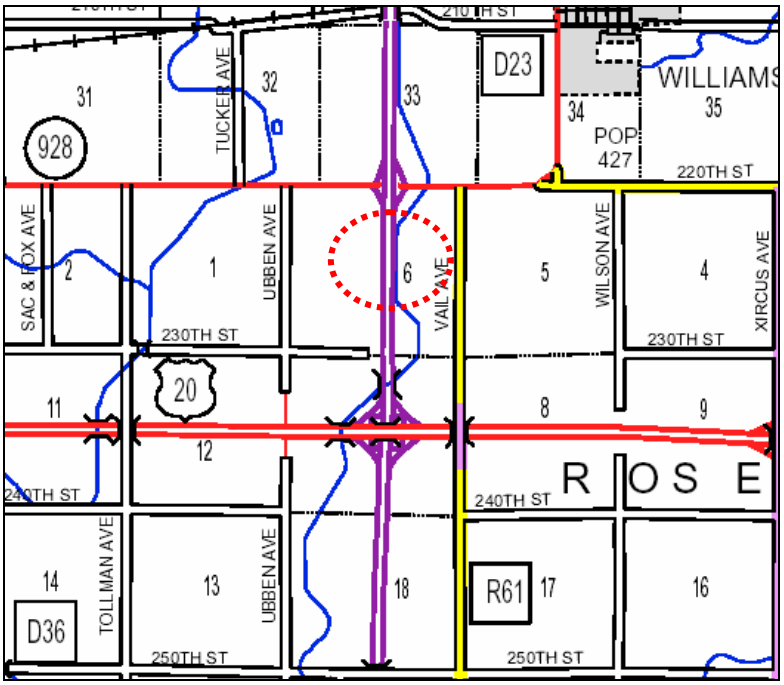

Figure 8. Location of project 9: Interstate 35 north of Highway 20

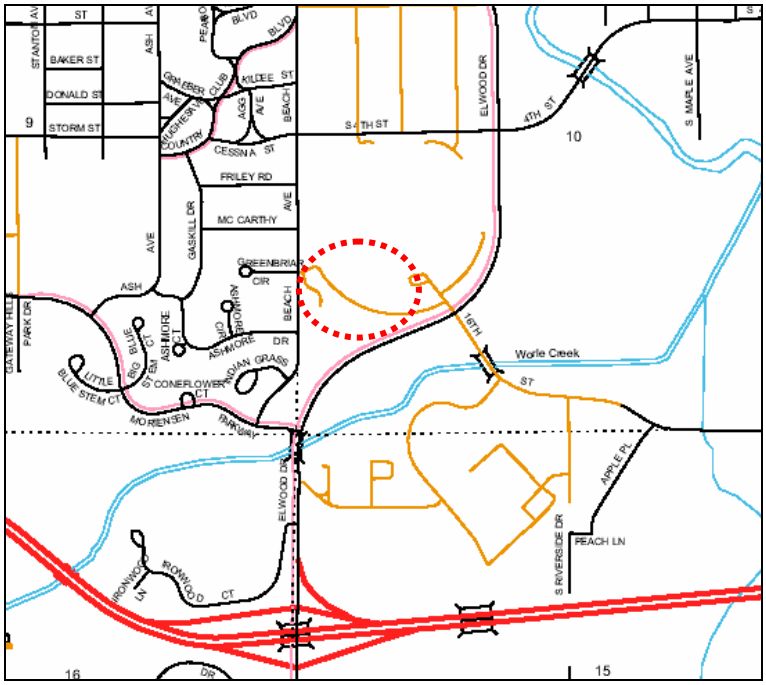

Figure 9. Location for projects 10 and 11: Ames, Iowa

Project 12

This project is located at the intersection of University and Guthrie Avenues in Des Moines, Iowa, along the I-235 reconstruction corridor. Testing was completed on special backfill in August 2003. The project location is shown in Figure 10.

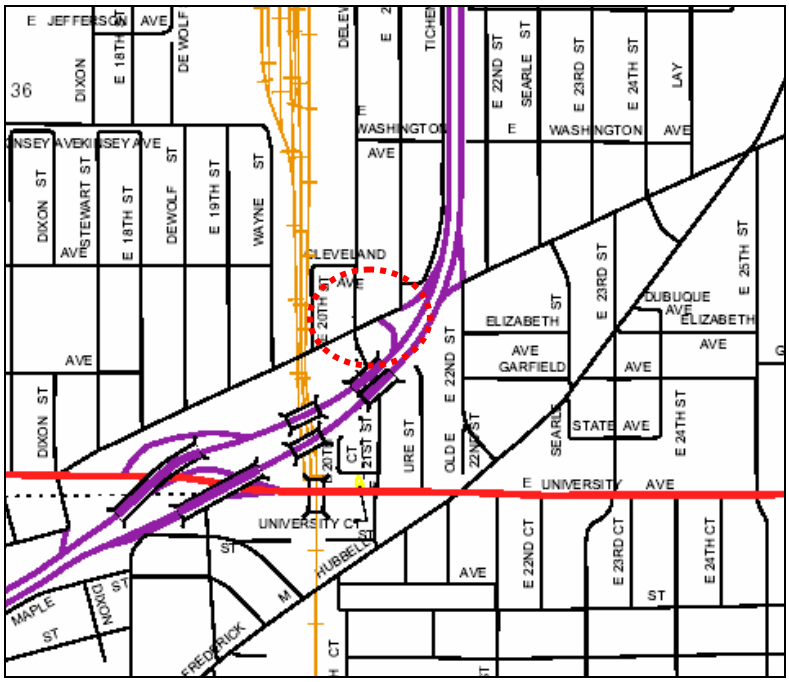

Figure 10. Location for project 12: University and Guthrie Aves, Des Moines, Iowa

Task 2: Grid Pavement and Document Pavement Quality

A grid was set out on the pavement surface prior to pavement removal to provide test locations and to document pavement distress locations. Table 1 shows a summary of all grid spacings for the field tests. Note that the X direction is perpendicular to the driving lane and the Y direction is parallel to the driving lane.

Task 3: DCP Testing

The DCP tests were conducted to measure the in situ strength of the subgrade/subbase site in terms of penetration resistance in mm/blow. DCP tests were conducted to a depth of about 450 mm. Figure 11 shows a DCP test being conducted.

Table 1. In situ test grid spacing

Project Number	Project Name	Number of Tests	Grid Spacing (ft)	
			X	Y
1	Eddyville Bypass	33	10	8
2	Highway 330	33	10	8
3	Knapp Street Subgrade	51	6	6
4	Knapp Street Subbase	24	6	6
5	35th Street Subgrade	130	4	4
6	35th Street Subbase	24	10	10
7	Highway 34	85	6	6
8	Highway 218	85	6	6
9	Interstate 35	85	6	6
10	Jack Trice Lot S1 Before Ash	18	10	8
11	Jack Trice Lot S1 After Ash	18	10	8
12	University-Guthrie Avenues	30	6	6

Task 4: Clegg Impact Hammer Testing

The Clegg Impact Hammer was used to obtain an in situ stiffness value. The Clegg test was chosen because it is quick and easy to conduct. The Clegg Impact Hammer is shown in Figure 12.

Task 5: GeoGauge Stiffness Testing

The GeoGauge stiffness test was used to determine the in situ modulus. The GeoGauge device is shown in Figure 13.

Figure 11. DCP testing on westbound entrance ramp of I-235 at 35th Street in West Des Moines, Iowa

Figure 12. Clegg Impact Hammer

Figure 13. GeoGauge

Task 6: Nuclear Density Gauge Testing

Nuclear density gauge readings were taken at each test point to determine its in situ dry density and moisture content. Tests were conducted to a depth of 300 mm. Figure 14 shows the nuclear density gauge used for testing.

Figure 14. Nuclear Density Gauge

Task 7: Determine Subgrade/Subbase Index Properties

To analyze the subgrade/subbase materials, the following index test methods were followed:

- ASTM D 422-63 (Standard Test Method for Particle-Size Analysis of Soils)
- ASTM D 2487-90 (Standard Test Method for Classification of Soil for Engineering Purposes)
- ASTM D 4318-84 (Standard Test for Liquid Limit, Plastic Limit, and Plasticity Index of Soils)

Upon completion of the subgrade/subbase in situ testing phase, the subgrade/subbase materials were sampled using two five-gallon plastic containers with lids. The samples were transported back to the laboratory where the samples were processed for testing.

Finite Element Modeling to Evaluate Pavement Response

Using the in situ test results, pavement systems were modeled using ISLAB2000, a powerful finite element analysis tool designed specifically for modeling rigid pavements. ISLAB2000 allows input parameter values for up to four layers in addition to the subgrade in an analysis. Outputs for the ISLAB2000 software are vertical deflections and stresses (x and y directions, shear stresses, and principal stresses). Deflections are measured in inches and stress is measured in pounds per square inch (psi).

For the purpose of this study, the pavement structure was modeled as a single layer. The pavement layer was modeled using the same PCC engineering properties for all cases while the subgrade/subbase was modeled on the in situ measured values (modulus of subgrade reaction values) using a Winkler spring foundation. Figure 15 illustrates the concept of the model with non-uniform subgrade/subbase stiffness.

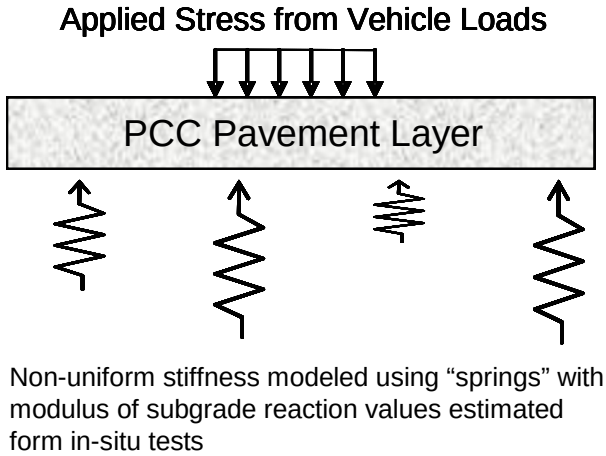

Figure 15. Winkler spring foundation to simulate non-uniform subgrade/subbase stiffness

Task 1: Estimate Modulus of Subgrade Reaction

As input for the numerical model, the modulus of subgrade reaction (k_s) was estimated from the in situ GeoGauge modulus values. The modulus values were first converted to English units and then the reduced Vesic equation (from Bowles 1996) was applied to estimate the modulus of subgrade reaction.

$$k_s = \frac{E_s}{B(1-\mu^2)} \qquad (1)$$

where the plate diameter, B, is assumed to equal 30 inches, Poisson's Ratio, μ, is assumed to be 0.35, and modulus values, E_s, are determined from the GeoGauge measurements. Upon estimating the modulus of subgrade reaction, the estimations were checked through various charts and graphs to ensure a reasonable approximation.

Task 2: Select Pavement Engineering Properties and Loading Conditions

Table 2 lists the variables included in the pavement model with their dimensions and engineering properties. These parameter values do not include all conditions, but provide some typical values for comparing the influence of non-uniformity in the subgrade stiffness. The only variables that did not remain constant throughout pavement modeling were the number of wheels, tire pressure, load, wheel spacing, and contact area.

Values estimated for load and vehicle purposes were derived from the American Association of State Highway Officials (AASHO) road test vehicles. With ever increasing axle configurations and weights, deviation from the AASHO road test should be considered in future analysis. In this effort, a few analyses were conducted using a standard 18-wheel tandem axle and a large farm grain cart configuration. Vehicle values for these two configurations are listed in Table 3. These configurations were modeled using data from Project 2 because this project showed high non-uniformity in subgrade stiffness.

With regard to load placement on PCC slabs, location creates a wide range of pavement responses, depending on subgrade characteristics and pavement type. For the purposes of this study, the loadings were placed at the corner and mid-span of each slab 18 inches from the pavement edge. In the future, additional load types and levels and load locations should be considered for a more comprehensive analysis.

Table 2. Input variables for ISLAB2000

Variable	Value
PCC Pavement Thickness (in.)	10.5
Deflection Load Transfer Efficiency (%)	980
PCC Layer Poisson's Ratio	0.15
PCC Modulus (psi)	4,000,000
PCC Unit Weight (lbs/in.^{3})	0.087
Number of Wheels	2
Tire Pressure (psi)	80
Tire Contact Area (in.^{2})	112.6
Wheel Spacing (in.)	96
Axle Load (lbs)	18,000

Table 3. Alternate axle design values

Model	Variable	Value
Grain Cart	Number of Wheels	2
	Tire Pressure (psi)	20
	Tire Contact Area (in.^{2})	700.1
	Wheel Spacing (in.)	165
	Axle Load (lbs)	28,000
18-Wheeler	Number of Wheels	4
	Tire Pressure (psi)	110
	Tire Contact Area (in.^{2})	38.7
	Wheel Spacing (in.)	102
	Tire to Tire Spacing	3
	Axle Load (lbs)	34,000

Task 4: Evaluate Pavement Responses

ISLAB2000 pavement responses were calculated and recorded for subsequent statistical analysis. For this study, the maximum principle stress and maximum deflection at the bottom of the slab was extracted from each numerical analysis model.

Upon initial analysis of each project, ISLAB2000 was used to determine the pavement responses associated with a perfectly uniform subgrade. A uniform subgrade was modeled to analyze the difference in results obtained from modeling a non-uniform subgrade to those obtained from modeling a uniform subgrade.

The average modulus of subgrade reaction value for each project was used in the modeling process, and the resulting pavement responses were determined and recorded for comparison.

Task 5: Estimate Pavement Life from Numerical Analysis Output

Pavement life was estimated by applying the ERES/COE equation to the ISLAB2000 results. Darter (1988) developed the ERES/COE equation from Army Corps of Engineers data.

$$\log N = 2.13\ SR^{-1.2} \qquad (2)$$

N is the number of repetitions to failure and SR is the stress ratio equal to the total tensile stress in the slab divided by the concrete modulus of rupture. Generally, if the SR is kept below 0.5, the number of repetitions to failure becomes infinite.

The number of repetitions to failure was then divided by an estimated number of repetitions per year, resulting in a pavement lifespan.

Statistical Analysis of Field and Numerical Results

Statistical analysis was completed on the field data and ISLAB2000 results to determine whether a meaningful relationship existed between subgrade variability and pavement performance.

Task 1: Determine the Mean, Standard Deviation, and COV Values for In-Situ Tests

The average, standard deviation, and COV were determined for each project using the DCP, nuclear density and moisture, GeoGauge stiffness, and Clegg impact values (CIV).

Task 2: Perform SAS Analysis of ISLAB2000 Results

Statistical analysis of the maximum principal stress and maximum deflection results was completed using SAS statistical analysis software. The results of the SAS analyses are mean, median, mode, standard deviation, coefficient of variation, and a test to determine whether the data is normally distributed. Results are calculated for the maximum principal stress and maximum deflections for each load location on every project. A complete discussion of these results is provided in Rupnow (2004).

MATERIALS

This section presents the in situ testing and laboratory analysis of the subgrade/subbase materials evaluated in this study. Field testing consisted of nuclear density gauge, GeoGauge, DCP, and Clegg Impact Hammer tests. Laboratory tests consisted of grain-size distribution and Atterberg limits test analysis of the subgrade/subbase materials. The complete results for all in situ tests are presented in the appendix.

In Situ Test Results

Nuclear Density Gauge

The average dry density and moisture content for each project test location are provided in Table 4. Also shown are the corresponding standard deviations and COV values. Note the low standard deviations for Projects 1 and 11, indicating that fly ash treatment reduced subgrade variability in terms of density and moisture content.

GeoGauge Stiffness

Table 5 lists the average modulus and stiffness values obtained from GeoGauge testing for each project. The GeoGauge results show increased stiffness for Projects 1 and 11, as well as the granular subbase tested for Project 12.

Dynamic Cone Penetrometer

The average mean DCP index values for each project are shown in Table 6. All tests were conducted to a depth of about 450 mm. In general, the results show that the DCP index tended to decrease for the stiffer materials at Projects 1, 11, and 12.

Clegg Impact Hammer

The average CIVs for each project are presented in Table 7. The Clegg Impact Hammer data show trends similar to the DCP and GeoGauge data. This is to be expected, as the CIV is also a measure of the soil stiffness.

Subgrade/Subbase Index Properties

For each subgrade/subbase sample, grain-size analysis and Atterberg limits tests were performed. The Unified Soil Classification System (USCS) group symbols and group name are provided for each sample in Table 8, organized by project.

Table 4. Summary of nuclear density gauge data for all projects

			Nuclear Density Gauge					
Project Number	**Project Name**	**Number of Tests**	**Average Moisture Content %**	**Standard Deviation**	**COV**	**Average Dry Density kg/m^3**	**Standard Deviation**	**COV**
1	Eddyville Bypass	33	9.5	0.67	7.0	1704	26.99	1.6
2	Highway 330	33	11.5	1.21	10.5	1919	29.16	1.5
3	Knapp Street Subgrade	51	15.3	3.35	21.8	1725	163.16	9.5
4	Knapp Street Subbase	24	10.4	0.86	8.3	1669	68.31	4.1
5	35th Street Subgrade	130	12.9	1.75	13.6	1868	46.89	2.5
6	35th Street Subbase	24	8.5	1.35	15.8	1815	120.37	6.6
7	Highway 34	85	7.1	0.96	13.4	2028	54.72	2.7
8	Highway 218	85	7.6	1.07	14.1	1990	56.34	2.8
9	Interstate 35	85	8.7	1.77	20.4	2012	83.14	4.1
10	Jack Trice Lot S1 Before Ash	18	8.1	1.06	13.0	1960	56.18	2.9
11	Jack Trice Lot S1 After Ash	18	8.8	0.89	10.1	1804	49.50	2.7
12	University-Guthrie Avenue	30	6.7	3.14	46.9	1640	81.23	5.0

Table 5. Summary of GeoGauge data for all projects

			GeoGauge Measurements					
Project Number	**Project Name**	**Number of Tests**	**Average Stiffness MN/m**	**Standard Deviation**	**COV**	**Average Modulus MPa**	**Standard Deviation**	**COV**
1	Eddyville Bypass	33	14.82	2.93	19.7	128.53	25.44	19.8
2	Highway 330	33	2.36	1.23	52.0	20.49	10.67	52.1
3	Knapp Street Subgrade	51	1.60	1.14	71.4	13.87	9.87	71.2
4	Knapp Street Subbase	24	9.54	1.55	16.2	82.77	13.44	16.2
5	35th Street Subgrade	130	4.72	0.95	20.1	40.91	8.08	19.8
6	35th Street Subbase	24	5.88	1.78	30.3	50.98	15.43	30.3
7	Highway 34	85	5.81	1.21	20.8	50.39	10.47	20.8
8	Highway 218	85	7.22	2.07	28.7	63.00	17.82	28.3
9	Interstate 35	85	4.68	1.11	23.8	40.95	9.35	22.8
10	Jack Trice Lot S1 Before Ash	18	9.65	1.58	16.4	83.73	13.73	16.4
11	Jack Trice Lot S1 After Ash	18	16.30	3.50	21.5	140.41	29.52	21.0
12	University-Guthrie Avenue	30	15.72	3.40	21.7	136.36	29.53	21.7

Table 6. Summary of DCP index data for all projects

Project Number	Project Name	Number of Tests	DCP Average Mean DCP Index mm/blow	DCP Standard Deviation	DCP COV
1	Eddyville Bypass	33	10.79	1.82	16.9
2	Highway 330	33	26.93	5.03	18.7
3	Knapp Street Subgrade	51	56.55	17.35	30.7
4	Knapp Street Subbase	24	20.77	4.15	20.0
5	35th Street Subgrade	130	34.22	7.17	20.9
6	35th Street Subbase	24	20.07	9.43	47.0
7	Highway 34	85	25.23	6.35	25.2
8	Highway 218	5	18.86	8.29	43.9
9	Interstate 35	85	37.29	9.99	26.8
10	Jack Trice Lot S1 Before Ash	18	20.81	2.98	14.3
11	Jack Trice Lot S1 After Ash	18	15.93	1.25	7.8
12	University-Guthrie Avenue	30	13.64	6.10	44.7

Table 7. Summary of CIVs for all projects

Project Number	Project Name	Number of Tests	Clegg Impact Hammer		
			Average CIV	Standard Deviation	COV
1	Eddyville Bypass	33	27.4	4.68	17.1
2	Highway 330	33	6.4	1.62	25.3
3	Knapp Street Subgrade	51	5.5	3.36	60.9
4	Knapp Street Subbase	24	23.5	3.12	13.3
5	35th Street Subgrade	130	6.2	2.01	32.4
6	35th Street Subbase	24	20.7	5.68	27.5
7	Highway 34	85	10.4	1.67	16.1
8	Highway 218	85	27.2	7.03	25.8
9	Interstate 35	85	9.3	3.82	41.2
10	Jack Trice Lot S1 Before Ash	18	21.6	4.04	18.7
11	Jack Trice Lot S1 After Ash	18	25.2	4.48	17.8
12	University-Guthrie Avenue	30	29.3	11.70	40.0

Table 8. USCS soil classifications for each project

Project Number	Project Name	USCS Symbol	USCS Group Name
1	Eddyville Bypass	GP-GM	Poorly Graded Gravel with Silt and Sand
2	Highway 330	SM	Silty Sand
3	Knapp Street Subgrade	SC	Clayey Sand
4	Knapp Street Subbase	GW-GM	Well Graded Gravel with Silt and Sand
5	35th Street Subgrade	CL	Lean Clay with Sand
6	35th Street Subbase	GP-GM	Poorly Graded Gravel with Silt and Sand
7	Highway 34	SM	Silty Sand
8	Highway 218	CL	Sandy Lean Clay
9	Interstate 35	CL-ML	Sandy Silty Clay
10	Jack Trice Lot S1 Before Ash	SC	Clayey Sand
11	Jack Trice Lot S1 After Ash	SM	Silty Sand with Gravel
12	University-Guthrie Avenue	GP-GM	Poorly Graded Gravel with Silt and Sand

RESULTS

This results discussion is divided into two sections: (1) numerical modeling results and (2) statistical analysis of the results. Each section details specific outcomes pertaining to that section.

Pavement Modeling

This section details results obtained from the pavement modeling process outlined in the methods section above. ISLAB2000 results show decreased pavement stress and deflection with increased subgrade stiffness due to the addition of self-cementing fly ash, HFA, or granular subbase. ISLAB2000 modeling of uniform subgrade shows a decrease in average pavement stress, deflection, and standard deviation for most projects.

ISLAB2000 Results

This section discusses results pertaining to the ISLAB2000 pavement modeling. The ISLAB2000 finite element modeling results show a few notable trends, including an overall general decrease in maximum principal stress and pavement deflection as the modulus of subgrade reaction increases. Past research shows this trend is to be expected. Figures 16 and 17 show an example of the output for project 1. For several loading locations, the principal stresses (Figure 16) and deflections (Figure 17) are shown. By viewing these results, it can be seen that the maximum principal stress developed varies as a function of the load placement location along the pavement. This is because the subgrade/subbase stiffness varies spatially under the pavement layer.

Comparisons between the non-uniform and uniform modeling results (see Tables 9 and 10) show a reduction in average maximum principal stress between non-uniform and uniform pavements. The uniform pavement subgrade/subbase (using the average value from in situ tests) ultimately performs better than that of the non-uniform pavement, since the pavement life is a function of the stress ratio. The stress ratio is reduced when the resulting pavement tensile stress is reduced. This then increases the number of repetitions to failure, leading to a longer service life.

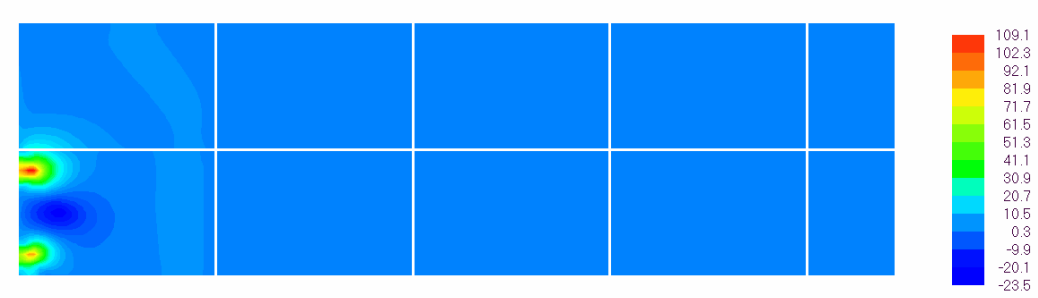
109.1
102.3
92.1
81.9
71.7
61.5
51.3
41.1
30.9
20.7
10.5
0.3
-9.9
-20.1
-23.5

(a)

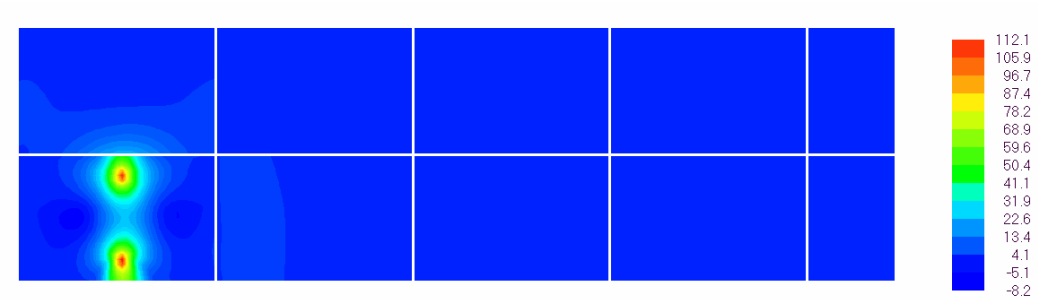
112.1
105.9
96.7
87.4
78.2
68.9
59.6
50.4
41.1
31.9
22.6
13.4
4.1
-5.1
-8.2

(b)

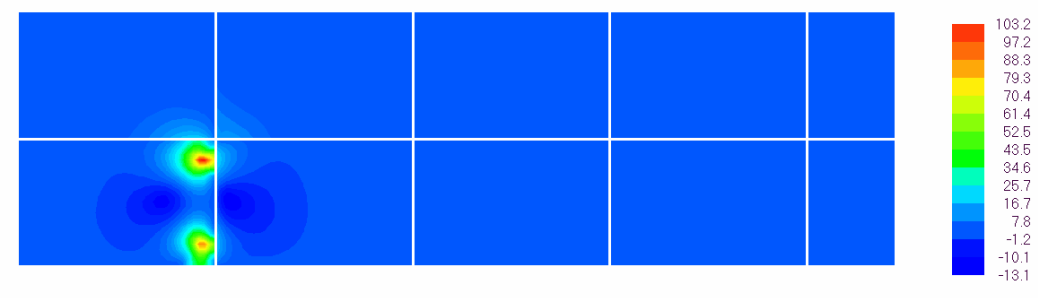
103.2
97.2
88.3
79.3
70.4
61.4
52.5
43.5
34.6
25.7
16.7
7.8
-1.2
-10.1
-13.1

(c)

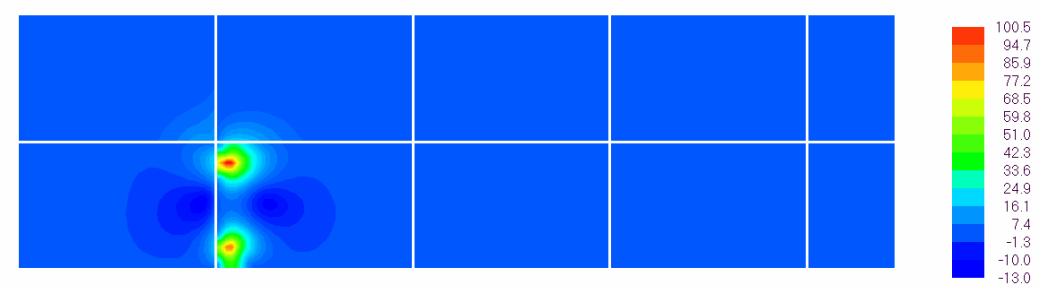
100.5
94.7
85.9
77.2
68.5
59.8
51.0
42.3
33.6
24.9
16.1
7.4
-1.3
-10.0
-13.0

(d)

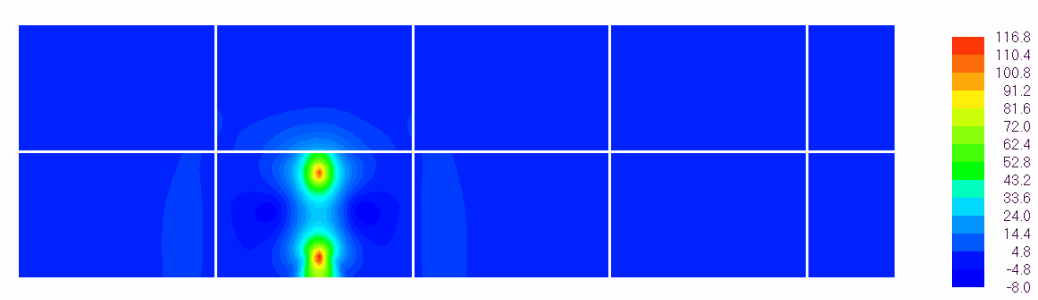
116.8
110.4
100.8
91.2
81.6
72.0
62.4
52.8
43.2
33.6
24.0
14.4
4.8
-4.8
-8.0

(e)

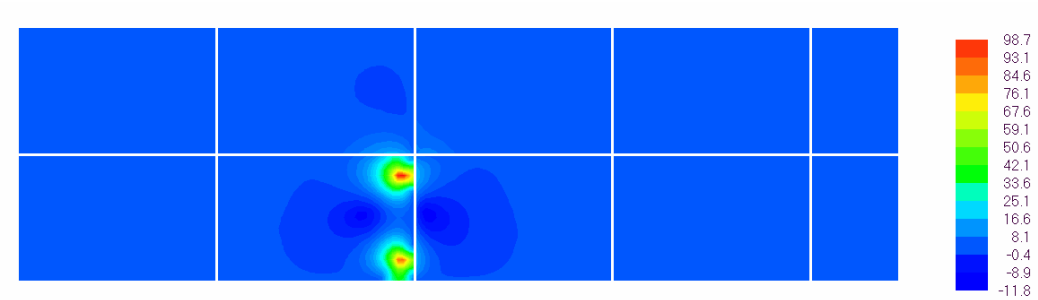
98.7
93.1
84.6
76.1
67.6
59.1
50.6
42.1
33.6
25.1
16.6
8.1
-0.4
-8.9
-11.8

(f)

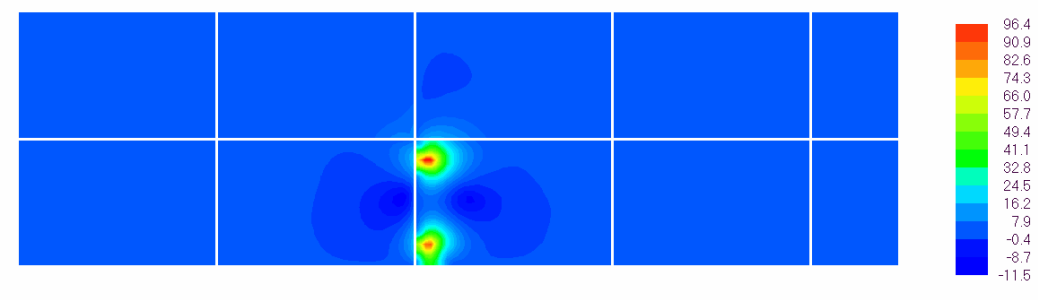
96.4
90.9
82.6
74.3
66.0
57.7
49.4
41.1
32.8
24.5
16.2
7.9
-0.4
-8.7
-11.5

(g)

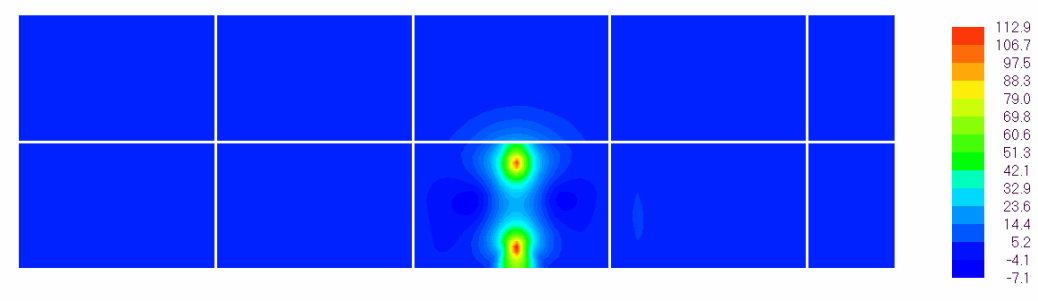
112.9
106.7
97.5
88.3
79.0
69.8
60.6
51.3
42.1
32.9
23.6
14.4
5.2
-4.1
-7.1

(h)

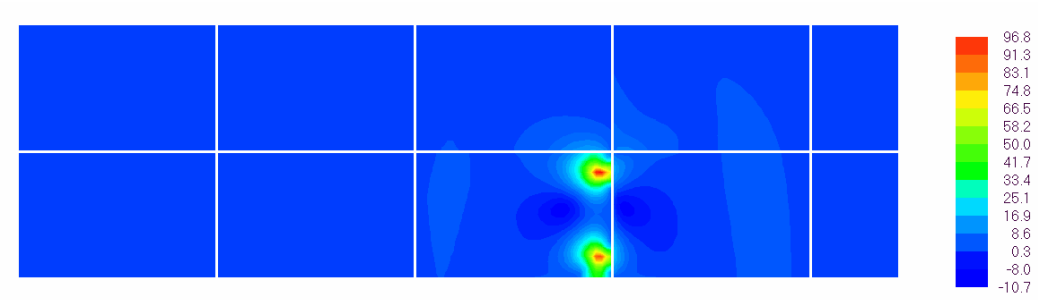
96.8
91.3
83.1
74.8
66.5
58.2
50.0
41.7
33.4
25.1
16.9
8.6
0.3
-8.0
-10.7

(i)

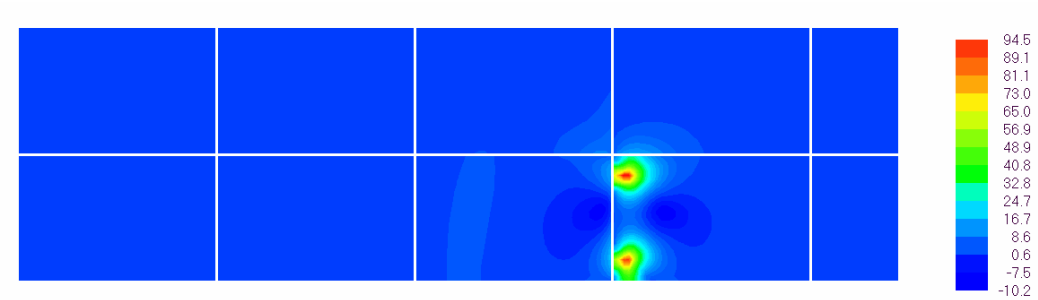
94.5
89.1
81.1
73.0
65.0
56.9
48.9
40.8
32.8
24.7
16.7
8.6
0.6
-7.5
-10.2

(j)

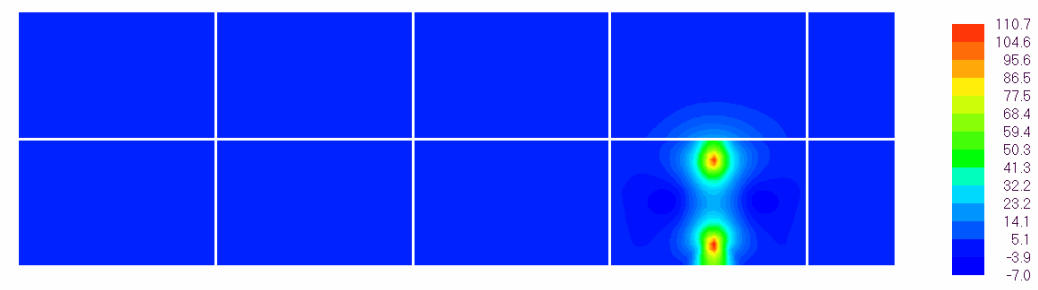
110.7
104.6
95.6
86.5
77.5
68.4
59.4
50.3
41.3
32.2
23.2
14.1
5.1
-3.9
-7.0

(k)

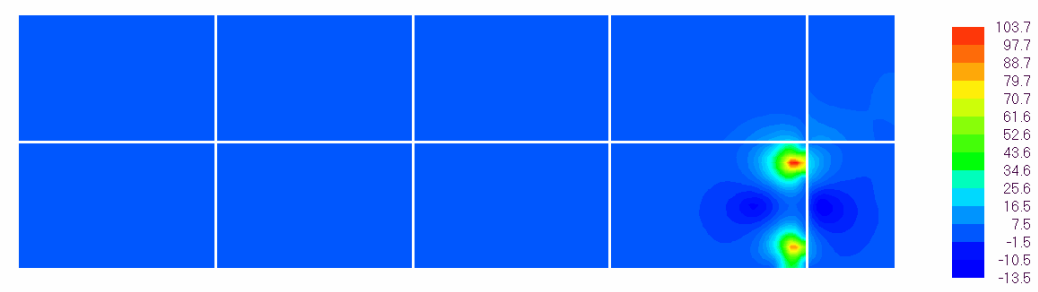
103.7
97.7
88.7
79.7
70.7
61.6
52.6
43.6
34.6
25.6
16.5
7.5
-1.5
-10.5
-13.5

(l)

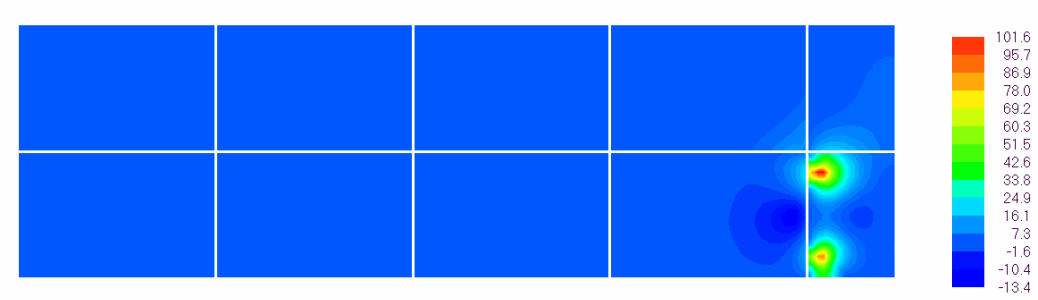

(m)

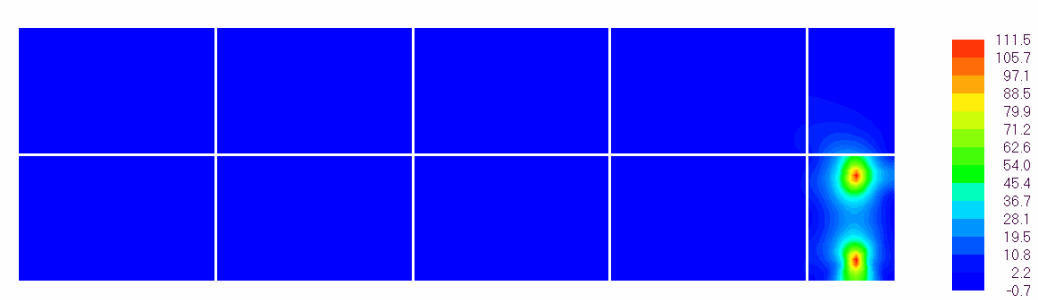

(n)

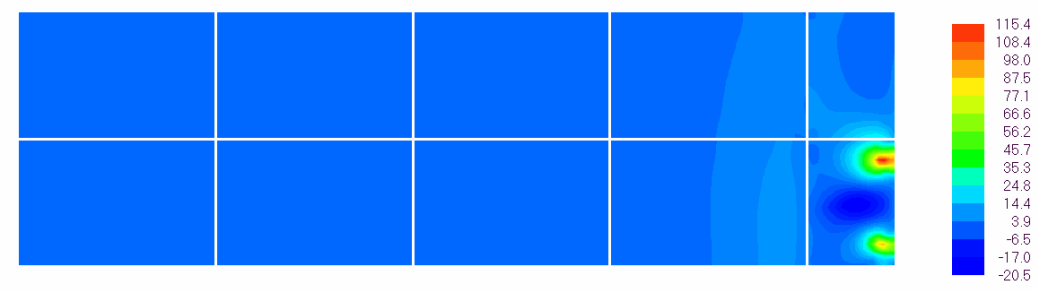

(o)

Figure 16. (a-o) Principle stress contours for each loading location for one lane of the Eddyville bypass (Project 1).

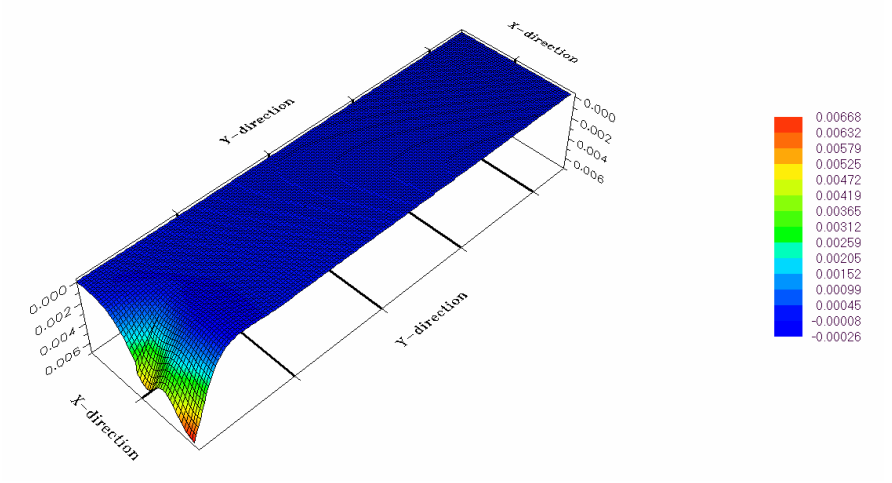
X-direction
Y-direction
0.000
0.002
0.004
0.006
Y-direction
0.000
0.002
0.004
0.006
X-direction
0.00668
0.00632
0.00579
0.00525
0.00472
0.00419
0.00365
0.00312
0.00259
0.00205
0.00152
0.00099
0.00045
-0.00008
-0.00026

(a)

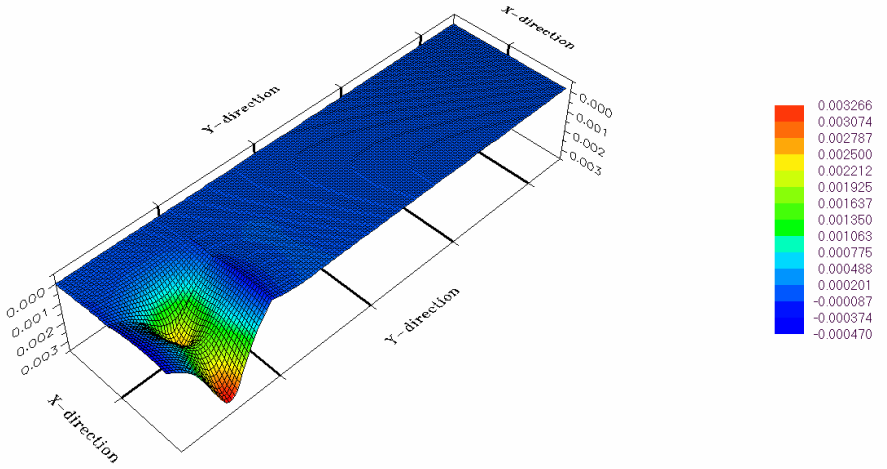
X-direction
Y-direction
0.000
0.001
0.002
0.003
Y-direction
0.000
0.001
0.002
0.003
X-direction
0.003266
0.003074
0.002787
0.002500
0.002212
0.001925
0.001637
0.001350
0.001063
0.000775
0.000488
0.000201
-0.000087
-0.000374
-0.000470

(b)

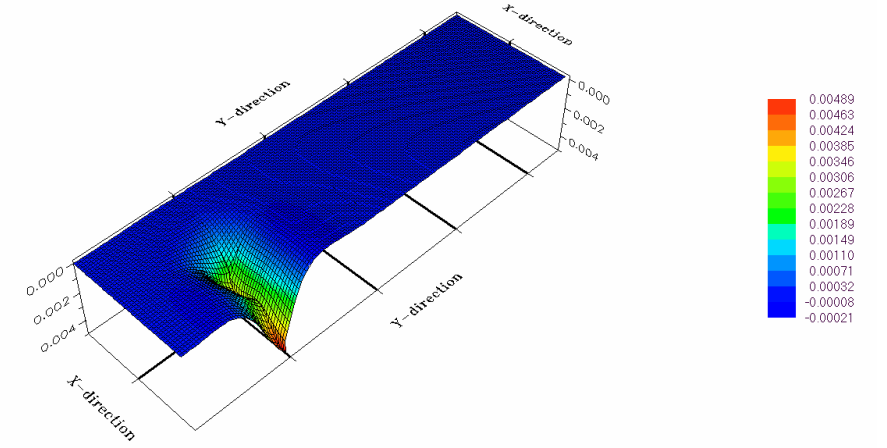
X-direction
Y-direction
0.000
0.002
0.004
Y-direction
0.000
0.002
0.004
X-direction
0.00489
0.00463
0.00424
0.00385
0.00346
0.00306
0.00267
0.00228
0.00189
0.00149
0.00110
0.00071
0.00032
-0.00008
-0.00021

(c)

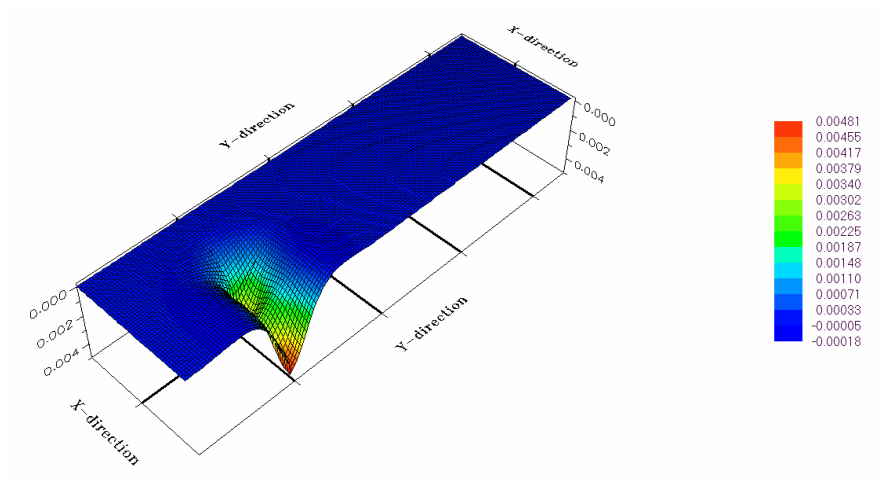
X-direction
Y-direction
0.000
0.002
0.004
0.000
0.002
0.004
Y-direction
X-direction
0.00481
0.00455
0.00417
0.00379
0.00340
0.00302
0.00263
0.00225
0.00187
0.00148
0.00110
0.00071
0.00033
-0.00005
-0.00018

(d)

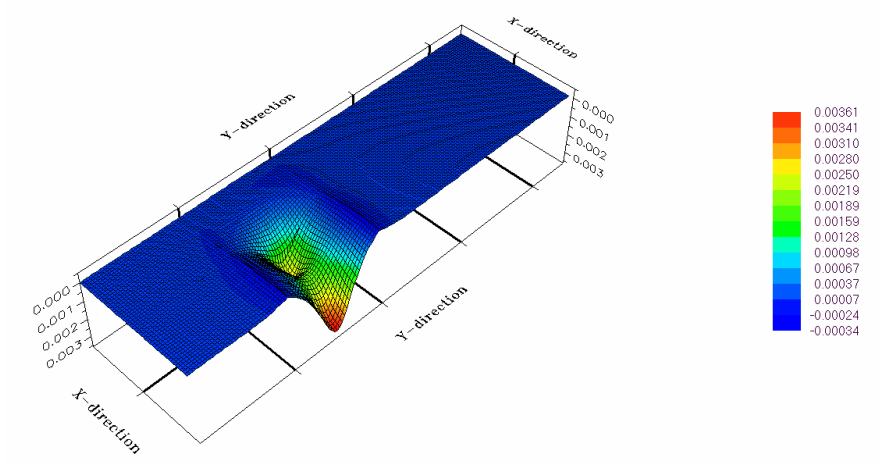
X-direction
Y-direction
0.000
0.001
0.002
0.003
0.000
0.001
0.002
0.003
Y-direction
X-direction
0.00361
0.00341
0.00310
0.00280
0.00250
0.00219
0.00189
0.00159
0.00128
0.00098
0.00067
0.00037
0.00007
-0.00024
-0.00034

(e)

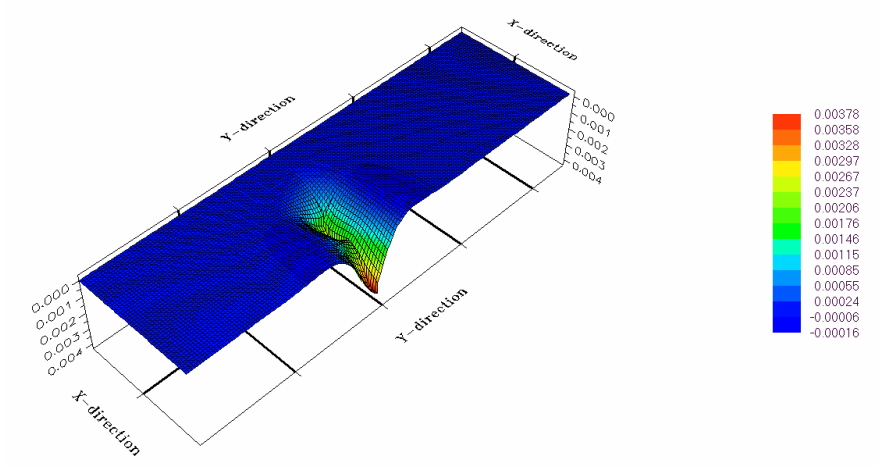
X-direction
Y-direction
0.000
0.001
0.002
0.003
0.004
0.000
0.001
0.002
0.003
0.004
Y-direction
X-direction
0.00378
0.00358
0.00328
0.00297
0.00267
0.00237
0.00206
0.00176
0.00146
0.00115
0.00085
0.00055
0.00024
-0.00006
-0.00016

(f)

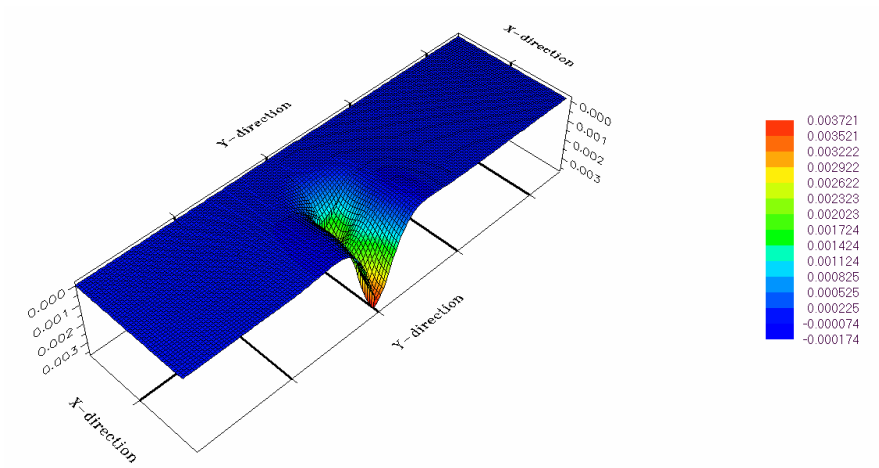
X-direction
Y-direction
0.000
0.001
0.002
0.003
Y-direction
X-direction
0.003721
0.003521
0.003222
0.002922
0.002622
0.002323
0.002023
0.001724
0.001424
0.001124
0.000825
0.000525
0.000225
-0.000074
-0.000174

(g)

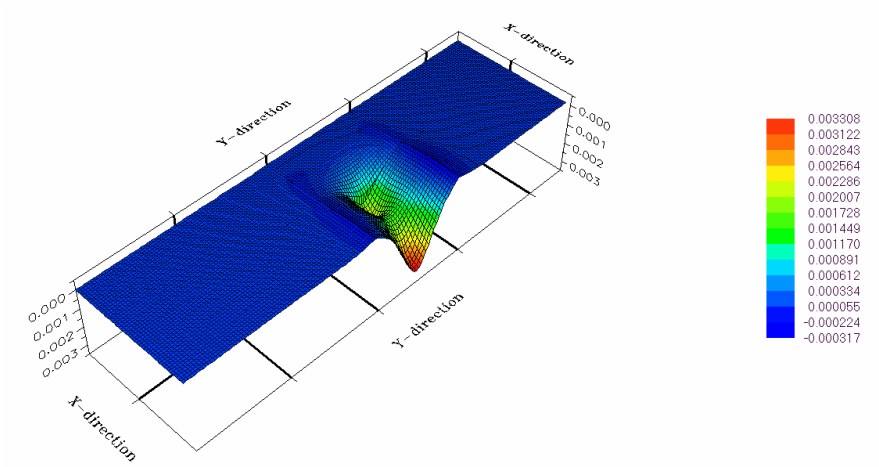
X-direction
Y-direction
0.000
0.001
0.002
0.003
Y-direction
X-direction
0.003308
0.003122
0.002843
0.002564
0.002286
0.002007
0.001728
0.001449
0.001170
0.000891
0.000612
0.000334
0.000055
-0.000224
-0.000317

(h)

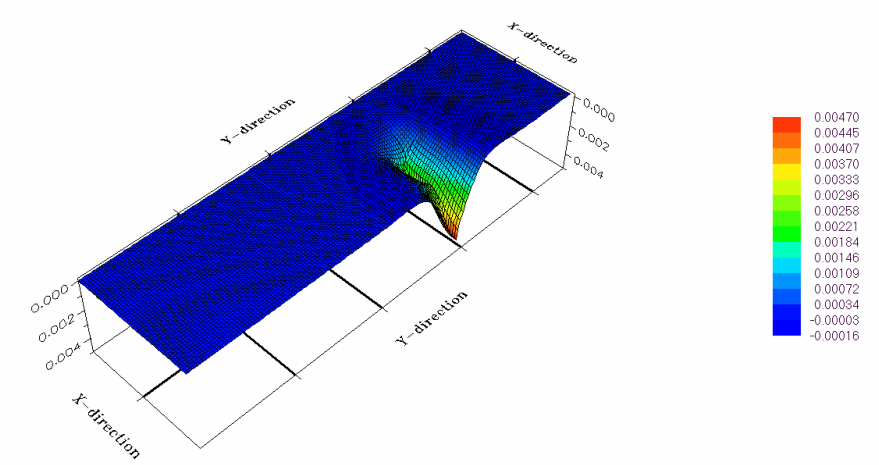
X-direction
Y-direction
0.000
0.002
0.004
Y-direction
X-direction
0.00470
0.00445
0.00407
0.00370
0.00333
0.00296
0.00258
0.00221
0.00184
0.00146
0.00109
0.00072
0.00034
-0.00003
-0.00016

(i)

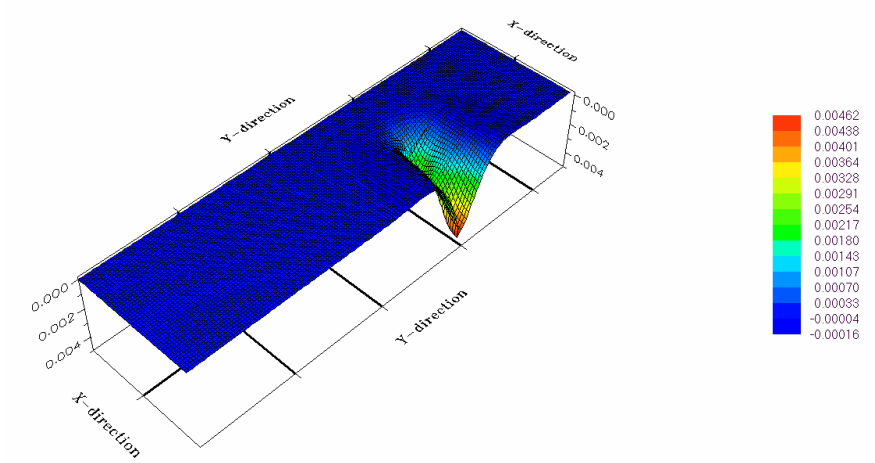
X-direction
Y-direction
0.000
0.002
0.004
Y-direction
0.000
0.002
0.004
X-direction
0.00462
0.00438
0.00401
0.00364
0.00328
0.00291
0.00254
0.00217
0.00180
0.00143
0.00107
0.00070
0.00033
-0.00004
-0.00016

(j)

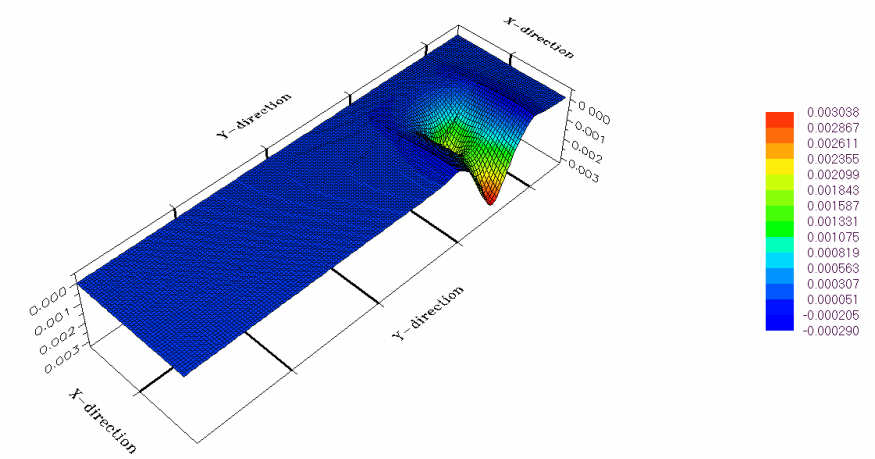
X-direction
Y-direction
0.000
0.001
0.002
0.003
Y-direction
0.000
0.001
0.002
0.003
X-direction
0.003038
0.002867
0.002611
0.002355
0.002099
0.001843
0.001587
0.001331
0.001075
0.000819
0.000563
0.000307
0.000051
-0.000205
-0.000290

(k)

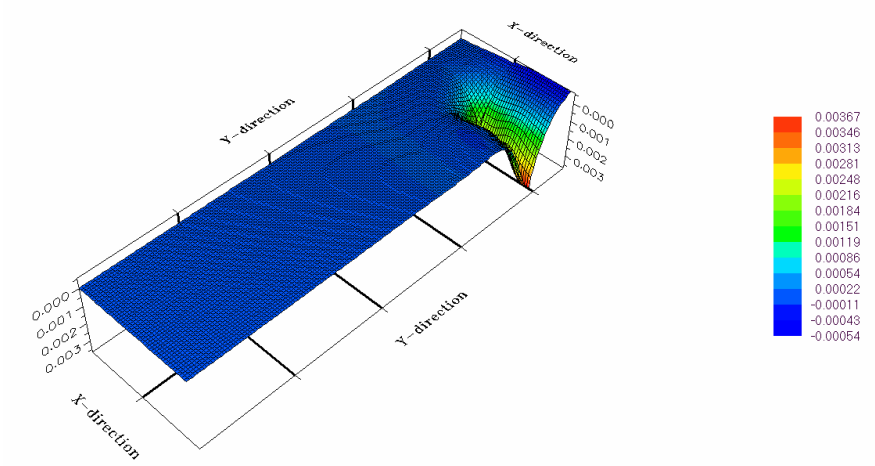
X-direction
Y-direction
0.000
0.001
0.002
0.003
Y-direction
0.000
0.001
0.002
0.003
X-direction
0.00367
0.00346
0.00313
0.00281
0.00248
0.00216
0.00184
0.00151
0.00119
0.00086
0.00054
0.00022
-0.00011
-0.00043
-0.00054

(l)

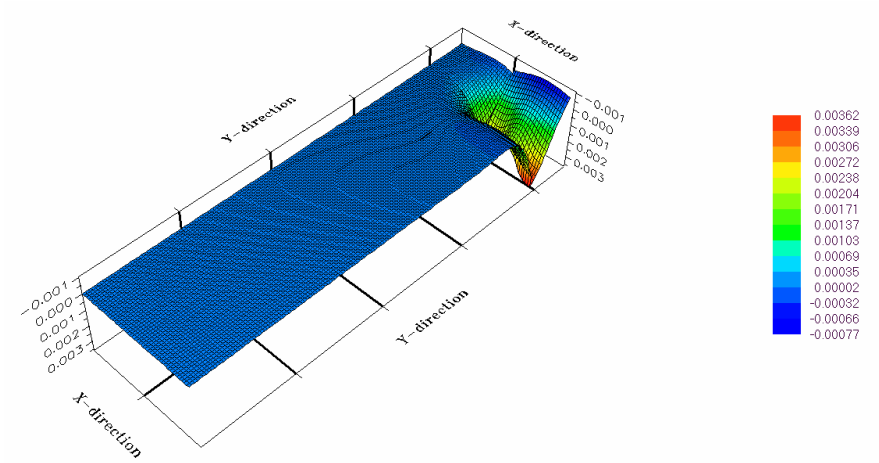

(m)

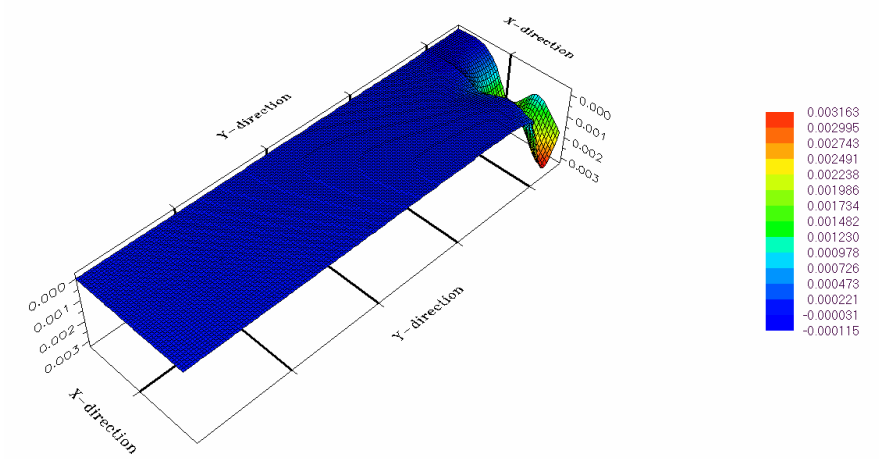

(n)

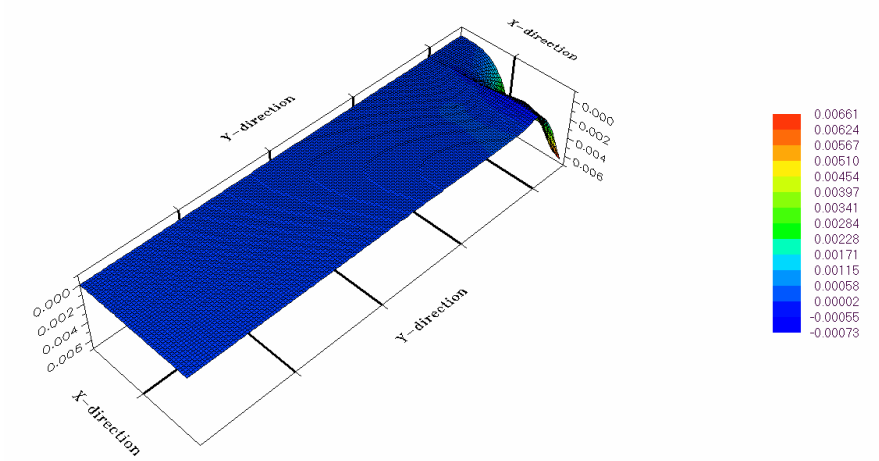

(o)

Figure 17. (a-o) Deflections for each loading location for one lane of the Eddyville bypass (Project 1).

Table 9 summarizes the project location and number, the number of ISLAB2000 test points, average maximum principal stress, average maximum deflections, and their respective standard deviations for the non-uniform analyses. Table 10 summarizes the project location and number, the number of ISLAB2000 test points, average maximum principle stress, average maximum deflections, and their respective standard deviations for the uniform analysis. For further information that includes individual output files on the individual principal stresses and deflections for a particular project, see Rupnow (2004).

Table 9. Average maximum principal stresses and deflections for all projects using the in situ measured results for non-uniform subgrade/subbase stiffness

			In Situ Measured (Non-Uniform) Subgrade/Subbase					
Project Number	**Project Name**	**Number of ISLAB2000 Test Points**	**Average Maximum Principal Stress kPa**	**Standard Deviation**	**COV**	**Average Maximum Deflection mm**	**Standard Deviation**	**COV**
1	Eddyville Bypass	40	722.33	45.96	6.36	0.111	0.064	57.10
2	Highway 330	40	855.55	156.19	18.26	0.549	0.320	58.28
3	Knapp Street Subgrade	16	820.93	128.52	15.66	0.396	0.171	43.11
4	Knapp Street Subbase	8	739.09	46.19	6.25	0.124	0.050	40.03
5	35th Street Subgrade	18	849.37	34.98	4.12	0.265	0.103	38.79
6	35th Street Subbase	12	848.56	71.33	8.41	0.163	0.068	42.00
7	Highway 34	32	725.90	129.44	17.83	0.252	0.107	42.64
8	Highway 218	32	715.60	125.31	17.51	0.225	0.098	43.77
9	Interstate 35	32	728.50	144.15	19.79	0.296	0.123	41.52
10	Jack Trice Lot S1 Before Ash	18	763.93	63.65	8.33	0.158	0.076	47.75
11	Jack Trice Lot S1 After Ash	8	729.64	41.83	5.73	0.103	0.045	44.16
12	University-Guthrie Avenue	6	777.32	32.20	4.14	0.148	0.068	45.58
13	Highway 330 with Grain Cart	40	1222.01	218.48	17.88	0.861	0.440	51.09
14	Highway 330 with 18-Wheeler	38	913.28	168.24	18.42	0.768	0.461	60.00

Table 10. Average maximum principal stresss and deflections for all projects using idealized uniform subgrade

			Idealized (Averaged) Uniform Subgrade/Subbase					
Project Number	**Project Name**	**Number of ISLAB2000 Test Points**	**Average Maximum Principal Stress (kPa)**	**Standard Deviation**	**COV**	**Average Maximum Deflection mm**	**Standard Deviation**	**COV**
1	Eddyville Bypass	40	712.19	55.78	7.83	0.110	0.040	36.44
2	Highway 330	40	847.88	141.84	16.73	0.464	0.180	38.83
3	Knapp Street Subgrade	16	818.66	107.14	13.09	0.361	0.156	43.12
4	Knapp Street Subbase	8	726.77	54.14	7.45	0.120	0.050	42.07
5	35th Street Subgrade	18	828.76	29.26	3.53	0.255	0.094	37.05
6	35th Street Subbase	12	832.68	72.98	8.76	0.156	0.066	42.13
7	Highway 34	32	705.51	130.93	18.56	0.231	0.094	40.51
8	Highway 218	32	693.16	117.02	16.88	0.195	0.078	40.27
9	Interstate 35	32	717.68	145.26	20.24	0.270	0.110	40.76
10	Jack Trice Lot S1 Before Ash	18	749.62	72.97	9.73	0.155	0.060	38.73
11	Jack Trice Lot S1 After Ash	8	712.86	54.66	7.67	0.103	0.039	38.06
12	University-Guthrie Avenue	6	779.24	12.34	1.58	0.130	0.045	34.44
13	Highway 330 with Grain Cart	40	1206.96	194.56	16.12	0.765	0.248	32.36
14	Highway 330 with 18-Wheeler	38	878.48	91.85	10.46	0.623	0.211	33.80

Pavement Life Results

Table 11 shows the number of repetitions to failure for each project for both the non-uniform and uniform subgrade modeling conditions. Note that simulation of a uniform subgrade produced a larger number of repetitions to failure for each project tested. This indicates that uniformity of subgrade influences pavement life.

Table 11. Number of repetitions to failure for all projects using non-uniform and uniform subgrade support values using ISLAB2000 finite element solution results

		In Situ Non-Uniform			Idealized Uniform		
Project Number	**Project**	**Average Maximum Principal Stress (kPa)**	**Standard Deviation**	**Number of Repetitions to Failure**	**Average Maximum Principal Stress (kPa)**	**Standard Deviation**	**Number of Repetitions to Failure**
1	Eddyville Bypass	722.33	45.96	3.80E+15	712.19	55.78	7.03E+15
2	Highway 330	855.55	156.19	5.20E+12	847.88	141.84	7.15E+12
3	Knapp Street Subgrade	820.93	128.52	2.30E+13	818.66	107.14	2.55E+13
4	Knapp Street Subbase	739.09	46.19	1.44E+15	726.77	54.14	2.92E+15
5	35th Street Subgrade	849.37	34.98	6.72E+12	828.76	29.26	1.63E+13
6	35th Street Subbase	848.56	71.33	6.95E+12	832.68	72.98	1.37E+13
7	Highway 34	725.90	129.44	3.08E+15	705.51	130.93	1.06E+16
8	Highway 218	715.60	125.31	5.70E+15	693.16	117.02	2.35E+16
9	Interstate 35	728.50	144.15	2.64E+15	717.68	145.26	5.03E+15
10	Jack Trice Lot S1 Before Ash	763.93	63.65	3.70E+14	749.62	72.97	7.98E+14
11	Jack Trice Lot S1 After Ash	729.64	41.83	2.47E+15	712.86	54.66	6.74E+15
12	University-Guthrie Avenue	777.32	32.20	1.85E+14	779.24	12.34	1.68E+14
13	Highway 330 with Grain Cart	1222.01	218.48	1.95E+08	1206.96	194.56	2.60E+08
14	Highway 330 with 18-Wheeler	913.28	168.24	5.73E+11	878.48	91.85	2.08E+12

Statistical Analysis

This section details results obtained from statistical analysis of the generated field data and ISLAB2000 pavement modeling data. Statistical analysis generally shows that HFA, self-cementing fly ash-treated subgrade, and granular subbases perform better with a smaller standard deviation and COV.

Field Data Statistical Analysis

The field data statistical analysis section is further broken down into the results for the nuclear density gauge, GeoGauge, Clegg Impact Hammer, and DCP. Each section discusses the results for each project with comparisons between projects.

Nuclear Density Gauge

Nuclear density gauge statistical analysis results, in Table 4, show several things. First, the results show wet subgrade soil conditions for project 3. Wet subgrade soil conditions were also encountered at projects 2 and 5. These three projects were all located under an existing PCC pavement placed on natural subgrade. With the absence of a drainage layer to expedite water removal, the soils became saturated.

The remaining projects show fairly uniform moisture contents ranging from about 6.5% to 10.5%. Note that increasing the number of test points does not necessarily decrease the standard deviation of the test results, as one would expect. Also note that one of the highest standard deviations occurs for Project 12, a granular subbase, which in theory is a more uniform material. Note that the standard deviation for Projects 1 and 11 are very low. This indicates good moisture uniformity.

GeoGauge

The GeoGauge data, in Table 5, show several results worth noting. First, there is a significant increase in stiffness from about 1.60 MN/m to about 16.30MN/m between natural subgrade soils and either fly ash-treated or granular base course materials. The same trend can be found in the modulus values. This result is to be expected, as the stabilized subgrade and granular subbase materials should be stiffer.

Note the high stiffness and modulus values for Projects 1, 11, and 12. This indicates that addition of self-cementing fly ash, HFA, or granular subbase increases the underlying support for pavements. Also note the low stiffness values for the saturated subgrade soils on Project 3.

One noteworthy observation is that the number of test points influences the standard deviation. The general trend is that the standard deviation is reduced with an increase in the number of data points. However, this trend does not hold true for all field data.

Dynamic Cone Penetrometer

DCP results (see Table 16) show a decrease in the mean DCP index as the material stiffness increases. The range of average mean DCP indices is about 56 mm/blow for subgrade soils on project 3 to about 10 mm/blow for the HFA material on project 1. These results follow logically with the stiffness data presented in the GeoGauge section.

Note that the greatest standard deviation of mean DCP index occurred on project 3, where the soils were saturated and showed the largest average mean DCP index. Also note the low mean

DCP index values for the HFA and granular subbases. One exception to these low DCP index values for the subgrade occurs on project 8, where the subgrade soil had been used as a haul road for earthwork construction. The DCP index correlates well with the GeoGauge and Clegg Impact Hammer results.

Clegg Impact Hammer

CIV data (Table 17) shows a trend similar to the GeoGauge and DCP data. As the CIV increases, the stiffness also increases and the mean DCP index decreases. The range of CIVs is from about 5.5 to about 29.3 for projects 3 and 12, respectively.

Notable observations include high CIVs on projects testing subbase, HFA, or self-cementing fly ash-treated soils. Exceptions to these observations include projects 8 and 10. Again, the section tested on project 8 was used as a haul road for several months during earthwork construction, and project 10 was tested in late summer, thus producing a subgrade that is stiffer due to a lack of moisture.

Note that low standard deviations occurred on some unlikely projects. One would think that project 1 would have a lower standard deviation due to the uniformity of the HFA used. The high subgrade modulus and corresponding modulus of subgrade reaction lead to reduced pavement stresses. The reduced pavement stresses should then lead to longer pavement life.

DISCUSSION

This section discusses the implications and applications of the findings detailed in the results section. The discussion section is divided into two parts: (1) pavement modeling and (2) statistical analysis.

ISLAB2000 Pavement Modeling

ISLAB2000 pavement modeling comparisons show a decrease in maximum principal stresses and pavement deflections as the modulus of subgrade reaction increases. Previous research shows that this is to be expected. Decreasing the pavement stresses under traffic loads prolongs the fatigue life of the pavement. This suggests that using self-cementing fly ash stabilization, a granular subbase, or an HFA base will improve long-term pavement performance.

An important point to consider is that geomaterials, such as soil and rock, behave very differently when saturated for extended periods of time. This leads the authors to note that the most critical pavement responses are expected when pavement foundations are tested during the spring thaw period. Soil stiffness and the modulus of subgrade reaction are key parameters studied that are influenced greatly by seasonal climate change. The softening of subgrade soil during the spring thaw would lead to increased pavement stresses and deflections.

Comparisons between the uniform and non-uniform subgrade support show that subgrade non-uniformity adversely affects pavement performance. However, increased pavement life shows that uniformly constructed subgrades will increase the number of repetitions to failure, ultimately leading to lower roadway maintenance costs.

Note that in modeling pavement systems for this study, all applied loads were placed 18 inches away from the edge of the pavement. The bending stresses in pavement structure would increase if the applied loads were placed immediately at the edge of the slab. This placement would decrease the pavement life significantly, due to the increased ratio between the modulus of PCC layer rupture and the maximum pavement bending stresses.

Voids can form underneath the pavement structure due to erosion, pumping, or localized settlement. This study did not investigate the effect of voids underneath PCC pavements. However, the corner loadings with voids would lead to higher pavement stresses and thereby reduce pavement life.

The results of this study show that uniform subgrades, as opposed to non-uniform subgrades, increase pavement life. Both sets of data show very high fatigue life. These numbers are high because of the level and gear configuration of the loads applied on the pavement systems. However, not every vehicle weighs 18,000 pounds and travels 18 inches from the pavement edge. Vehicles traveling closer to the pavement edge would considerably increase the pavement bending stresses and thus significantly reduce pavement life.

Statistical Analysis

Field Data Statistical Analysis

The coefficient of variation (COV) values show that variability is significantly reduced with the addition of a granular subbase and self-cementing fly ash-stabilized subgrade. The HFA base used in project 1 also shows low variability. The low variability exhibited by these materials will increase confidence in the pavement design.

Decreasing variability allows the pavement designer to reduce the safety factor in pavement design, allowing for some cost saving measures to be undertaken, such as reduction in granular subbase thickness, base thickness in asphalt design, or PCC pavement thickness.

The pavement designer could opt to keep a pocket factor of safety in the design by basing the pavement design upon a more variable subgrade, thus increasing the pavement life and reducing the cost to taxpayers.

ISLAB2000 Statistical Analysis

Attempts to fit the ISLAB2000 results to a distribution failed, suggesting that the data is not beta or normally distributed. If the data were normally distributed, the pavement design could be made more efficient by using a percentage of the distributed stress in the pavement design. This would allow for a better pavement design, which would allow the designer to determine the feasible stress level for design.

Basing the design on stresses allows for a better designed pavement. The AASHTO 2002 Design Guide will have a mechanistic-empirical design philosophy based on pavement stresses combined with traditional empirical design. Current design practices use equivalent single axle loads (ESALs) for design. The main drawback is that determining the amount of ESALs can be difficult. Using stress to calculate the number of repetitions to failure may allow for better design, provided the years of service life are calculated using appropriate growth factors.

The variability reduction shown when pavement was modeled using a uniform subgrade shows that non-uniformity does factor into pavement performance. A uniform subgrade shows longer pavement life through less variability in pavement stresses.

The increase in reliability through the use of a uniform subgrade will allow pavement designers to determine more economic designs in the future. The pavement life will also increase due to the reduced pavement stresses attributed to the uniform subgrade.

SUMMARY AND CONCLUSIONS

This project attempted to link subgrade/subbase non-uniformity and pavement performance. This project set forth three objectives:

1. Generate field data from 10 to 12 local subgrade or pavement reconstruction projects in Iowa
2. Using field data, develop numerical models to simulate pavement performance in terms of critical pavement responses of bending stresses and deflections
3. Conduct statistical analysis of the results to determine whether a correlation exists between pavement life and subgrade non-uniformity

Some of the key findings of this research follow:

- Some recognized, direct causes of subgrade/subbase non-uniformity include (1) expansive soils, (2) differential frost heave and subgrade softening, (3) non-uniform strength and stiffness due to variable soil type, moisture content, and density, (4) pumping and rutting, (5) cut/fill transitions, (6) poor grading, and (7) gaps/voids underneath the pavement structure.

- Previous research finds that design k-values should be top of embankment rather than top of base k-values because (1) top of base k-values are unreasonably high and not recommended for design and (2) soil transmits its variance gradually to the pavement surface (Grabe 1993).

- Relative compaction alone is not enough to ensure pavement performance, but the subgrade soils stiffness must be measured and controlled (Sargand *et al.* 2000).

- For this project, field data were generated to provide technical data that could generate subgrade support values to be used in finite element modeling that would evaluate pavement performance. Field data were generated by using a grid system and conducting several in situ tests at each grid point.

- In situ testing of the subgrade revealed that moisture contents, density, stiffness, and the strength of natural subgrade soils are more variable and weaker than fly ash-stabilized subgrade, reclaimed hydrated fly ash subbase, and granular subbase.

- Nuclear density gauge results show that wet subgrade soil conditions were encountered on old PCC pavement projects that had been placed directly on natural subgrade soil. In the absence of a drainage layer to facilitate water removal, the soils became saturated. Poor draining pavement foundations cause instability in the unbound base materials and intensify the pumping in the subgrade layer.

- Higher stiffness and modulus values were measured on projects using self-cementing fly ash, reclaimed hydrated fly ash subbase, or granular subbase. Lower stiffness values were measured for projects with saturated subgrade soils.

- Comparisons between the non-uniform and uniform modeling results show a reduction in average maximum bending/principal stresses for the uniform subgrade/subbase conditions. Furthermore, the simulation of a uniform subgrade produced a larger number of repetitions to fatigue failure for each project tested. This indicates that subgrade uniformity directly influences pavement performance.

- ISLAB2000 pavement modeling comparisons show a decrease in maximum bending/principal stresses and decrease in pavement deflection as the modulus of subgrade reaction increases.

- Decreasing the pavement stresses under traffic loads increases pavement life. This indicates that using improved subgrade/subbase support (e.g. self-cementing fly ash stabilization, reclaimed hydrated fly ash subbase, or granular subbase) will improve pavement performance. Decreasing the stresses in the PCC slab will also allow better performing, smoother, and longer lasting concrete pavements.

- Conclusions of the research confirm that a link exists between pavement performance and subgrade non-uniformity. Finite element modeling results indicate that a uniform subgrade reduces critical pavement responses, such as stresses and deflections, leading to improved pavement life. Statistical analysis (of mean and COV values) shows that field results for self-cementing fly ash-treated subgrade, reclaimed hydrated fly ash, and granular subbase tend to be more uniform and have higher stiffness than Iowa soil subgrades.

- This study did not investigate the effect of voids underneath PCC pavement. However, corner loadings with voids could lead to higher pavement stresses and deflections, thereby reducing pavement life.

- The major conclusion of this study is that pavement performance is adversely affected by non-uniform subgrade support. Pavement life can be increased through the use of more uniform subgrade support. Providing a uniform subgrade/subbase support should be considered in the future as one of the key issues in achieving long lasting and better performing pavement systems. Achieving uniformity in pavement foundation will require improvements to be made in construction methods and field quality control testing.

REFERENCES

American Concrete Pavement Association. (2001). Professor's Seminar, Engineering of Concrete Pavements, A Seminar for Civil Engineering Educators, Skokie, Illinois, June 18-20, 2001.

American Concrete Pavement Association. (1995). Subgrades and Subbases for Concrete Pavements, Concrete Paving Technology, TB011.02P.

Bowles, J. (1996). *Foundation analysis and design*. McGraw-Hill, New York.

Darter, M., Hall, K., and Kuo, C. (1995). "Support under Portland cement concrete pavements." *National Cooperative Highway Research Program Report 372*, Transportation Research Board, Washington, D.C.

Grabe, J. (1993). "Spatial variation of soil stiffness: Spectral density approach." *Soil Dynamics and Earthquake Engineering* (13), Great Britain.

Huang, Y. (2004). *Pavement analysis and design*. Pearson Prentice Hall, New Jersey.

Ioannides, A. (1984). "Analysis of slabs-on-grade for a variety of loading and support conditions." PhD. Dissertation, University of Illinois, Urbana, IL.

Khazanovich, L. (1994). "Structural analysis of multi-layered concrete pavement systems." PhD. Dissertation, University of Illinois, Urbana, IL.

Sargand, S., Masada, T., Wasniak, D. (2000). "Constructing and controlling compaction of earth fills." *ASTM STP 1384*, American Society for Testing and Materials, West Conshohocken, PA.

SHRP. (1990). Distress identification manual for the long-term pavement performance studies. Strategic Highway Research Program, National Research Council, Washington, D.C.

Rupnow, T. D. (2004). "Influence of Subgrade Improvement and Non-uniformity on Pavement Performance," Iowa State University, M.S. Thesis.

Yoder, E.J. (1959). *Principles of Pavement Design*, John Wiley & Sons, Inc., New York.

APPENDIX – IN SITU TESTING RESULTS

Project 1	Eddyville Bypass
Date	4-Sep

	Coordinates		Nuc Gage Results			600 mm		300 mm		Geogage			
Test #	X	Y	% Moisture	Dry Density	CIV	Mean DCP Index, mm/blow	Mean Change in DCP Index, mm/blow	Mean DCP Index, mm/blow	Mean Change in DCP Index, mm/blow	Stiffness	Modulus	% Moisture Lab	CBR
1	0	-8	9.7	1689	22.6	10.73	2.25	6.56	1.56	16.49	143.06	20.0	35.5
2	0	0	8.8	1682	27.2	11.76	2.74	8.86	2.31	12.60	109.28	18.8	25.4
3	0	8	9.8	1748	29.2	9.93	2.24	6.42	0.08	16.24	140.84	20.5	36.4
4	10	-8	9.0	1736	30.5	10.65	2.96	5.62	0.92	11.58	100.46	19.2	42.2
5	10	0	8.5	1712	28.4	12.50	4.32	6.52	1.96	9.46	81.11	19.5	35.8
6	10	8	9.7	1681	22.8	10.64	3.92	7.89	3.35	19.59	169.95	21.1	28.9
7	20	-8	9.0	1665	25.5	16.07	5.02	7.67	0.02	11.76	102.01	19.1	29.8
8	20	0	9.4	1713	28.4	11.97	2.60	6.67	0.74	10.80	93.70	18.6	34.9
9	20	8	8.9	1714	18.5	9.32	2.30	8.07	1.75	20.57	178.48	19.1	28.2
10	30	-8	10.7	1744	24.9	9.95	2.00	5.16	0.80	16.43	142.57	19.7	46.5
11	30	0	9.2	1721	29.1	9.73	3.82	6.46	2.28	17.91	155.35	20.1	36.1
12	30	8	9.4	1667	20.7	15.31	1.87	7.90	1.42	9.23	80.03	18.9	28.8
13	40	-8	10.8	1706	26.0	9.21	2.81	4.82	0.70	14.08	122.16	20.8	50.2
14	40	0	10.3	1694	29.7	12.64	2.19	6.30	0.53	15.87	137.64	21.1	37.2
15	40	8	9.0	1684	22.9	11.92	3.99	6.77	2.98	15.14	131.32	16.6	34.3
16	50	-8	9.7	1707	24.1	8.36	2.50	5.94	1.03	12.34	107.08	20.9	39.7
17	50	0	8.8	1697	37.7	12.30	2.41	7.55	2.01	18.61	161.48	21.5	30.3
18	50	8	8.9	1696	22.4	12.88	4.79	6.59	1.40	11.14	96.64	20.5	35.3
19	60	-8	10.3	1713	36.3	9.90	2.51	6.19	4.63	15.81	137.13	21.7	37.9
20	60	0	9.2	1703	26.7	12.58	2.64	8.61	0.55	14.52	125.95	19.5	26.2
21	60	8	10.4	1750	36.0	9.26	1.98	4.63	1.21	18.30	158.79	20.1	52.5
22	70	-8	9.5	1719	26.3	11.76	1.64	6.04	4.13	17.30	150.11	18.9	39.0
23	70	0	8.7	1694	27.4	9.36	2.26	6.04	0.76	9.95	86.28	18.9	39.0
24	70	8	9.0	1696	32.0	10.79	3.11	6.26	4.47	15.55	134.86	18.9	37.4
25	80	-8	10.1	1694	24.1	11.12	4.46	7.66	2.92	16.29	141.34	20.4	29.9
26	80	0	10.1	1687	31.1	10.60	3.04	5.33	1.04	14.88	129.07	20.9	44.8
27	80	8	8.9	1686	27.5	8.64	1.17	6.79	2.32	14.06	121.96	18.9	34.2
28	90	-8	8.7	1773	21.8	9.56	1.98	6.72	4.80	13.50	117.14	19.9	34.6
29	90	0	8.9	1713	29.9	9.49	2.61	6.97	2.61	14.96	129.77	20.7	33.2
30	90	8	9.9	1728	29.6	8.94	2.58	6.18	1.36	14.91	129.31	20.4	38.0
31	100	-8	9.3	1692	21.0	10.17	1.01	6.48	1.34	14.07	122.07	19.3	36.0
32	100	0	10.1	1655	34.0	8.45	2.06	6.49	1.30	16.97	147.24	20.6	35.9
33	100	8	10.8	1657	30.3	9.62	2.38	5.71	0.74	18.14	157.39	20.4	41.5
	Average		9.5	1704	27.4	10.79	2.73	6.60	1.82	14.82	128.53	19.9	36.2
	Standard Deviation		0.67	26.99	4.68	1.82	0.98	1.00	1.30	2.93	25.44	1.05	6.29

Project 2	Hwy 330
Date	9/14/2002

	Coordinates		Nuc Gage Results			600 mm		300 mm		Geogage		
Test #	X	Y	% Moisture	Dry Density	CIV	Mean DCP Index, mm/blow	Mean Change in DCP Index, mm/blow	Mean DCP Index, mm/blow	Mean Change in DCP Index, mm/blow	Stiffness	Modulus	CBR
1	0	-8	9.1	1929	10.6	23.79	6.02	37.75	8.00	4.29	37.23	5.0
2	0	0	13.2	1890	5.6	40.07	6.57	47.57	6.67	2.45	21.27	3.9
3	0	8	11.5	1909	5.3	22.26	5.19	30.00	8.00	2.88	25.02	6.5
4	10	-8	9.2	1938	7.6	16.40	3.40	31.10	5.89	4.06	35.22	6.2
5	10	0	9.9	1996	5.9	26.48	5.05	32.10	5.11	4.92	42.66	6.0
6	10	8	13.4	1902	6.0	26.30	5.45	44.29	9.67	1.01	8.77	4.2
7	20	-8	10.0	1944	5.2	22.70	4.38	32.80	7.89	1.90	16.45	5.9
8	20	0	13.2	1928	6.0	30.50	5.00	38.25	6.00	2.59	22.49	4.9
9	20	8	11.8	1930	4.1	32.26	5.72	37.00	7.88	0.45	3.95	5.1
10	30	-8	11.2	1898	5.6	27.30	7.68	38.38	13.29	2.91	25.27	4.9
11	30	0	11.1	1945	5.2	25.08	7.26	38.50	10.43	1.55	13.41	4.9
12	30	8	11.2	1958	9.0	24.72	4.13	24.46	3.42	3.42	29.69	8.1
13	40	-8	10.1	1904	10.4	20.25	9.18	35.33	14.13	3.44	29.83	5.4
14	40	0	11.7	1902	5.3	22.56	5.30	37.75	9.00	2.24	19.42	5.0
15	40	8	13.0	1929	6.8	26.30	5.95	25.50	5.45	3.62	31.43	7.8
16	50	-8	9.8	1928	4.7	26.74	5.30	32.22	5.13	1.16	10.03	6.0
17	50	0	13.3	1876	4.9	25.62	3.93	41.13	6.14	1.28	11.10	4.5
18	50	8	11.5	1936	5.0	31.79	8.06	33.67	7.75	2.07	18.00	5.7
19	60	-8	11.5	1946	9.0	32.21	7.72	39.13	8.00	4.43	38.46	4.8
20	60	0	10.8	1895	5.3	31.79	7.06	45.57	10.17	0.10	0.83	4.1
21	60	8	11.0	1935	4.6	26.09	7.82	30.50	9.89	2.55	22.14	6.4
22	70	-8	10.5	1941	7.8	28.43	4.55	37.57	3.57	1.88	16.27	5.0
23	70	0	12.6	1918	7.7	17.59	3.32	27.73	6.10	2.52	21.90	7.1
24	70	8	12.2	1902	5.9	25.29	6.09	29.90	6.33	2.33	20.21	6.5
25	80	-8	12.7	1920	5.5	24.60	4.08	26.92	2.55	0.78	6.75	7.3
26	80	0	10.2	1981	7.1	23.23	3.12	30.10	4.00	1.90	16.25	6.4
27	80	8	11.9	1922	7.2	21.94	7.44	30.50	10.33	2.42	21.02	6.4
28	90	-8	12.6	1863	6.7	30.50	6.00	34.67	7.88	2.11	18.29	5.5
29	90	0	12.2	1917	7.4	27.55	4.76	25.25	4.27	2.25	19.52	7.8
30	90	8	10.5	1873	5.5	35.61	7.00	36.00	7.88	0.99	8.59	5.3
31	100	-8	12.2	1886	5.6	33.67	11.18	44.86	12.83	0.82	7.16	4.1
32	100	0	12.0	1898	7.3	28.90	5.50	25.83	4.36	4.56	39.55	7.7
33	100	8	12.2	1901	5.0	30.20	6.95	31.80	6.89	2.08	18.03	6.1
	Average		11.5	1919	6.4	26.93	5.94	34.37	7.42	2.36	20.49	5.8
	Standard Deviation		1.21	29.16	1.62	5.03	1.78	6.17	2.85	1.23	10.67	1.16

Project 3	Knapp Street Ames, IA
Date	5/21/2003

	Coordinates		Nuc Gage Results			450 mm		300 mm		150 mm	Geogage		
Test #	X	Y	% Moisture	Dry Density, kg/m^3	CIV	Mean DCP Index, mm/blow	Mean Change in DCP Index, mm/blow	Mean DCP Index, mm/blow	Mean Change in DCP Index, mm/blow	Mean DCP Index, mm/blow	Stiffness, MN/m	Modulus, kPa	CBR
1	0	-15	13.4	1716	2.4	86.06	20.67	94.75	30.50	110.00	1.36	11.79	1.8
2	0	-9	15.1	1765	7.5	49.22	11.17	54.71	3.92	52.75	3.06	26.58	3.3
3	0	-3	14.7	1723	10.9	39.93	28.60	43.00	32.00	27.00	3.16	27.44	4.3
4	0	-3	12.4	1724	10.9	37.11	26.83	41.58	26.83	28.17	2.52	21.90	4.5
5	0	-9	11.4	1942	4.9	52.84	16.07	62.17	8.33	66.33	2.22	19.24	2.9
6	4	-15	13.9	1819	2.2	73.08	25.88	87.75	15.50	95.50	2.15	18.65	1.9
7	4	-15	14.8	1858	1.2	87.13	82.64	119.33	137.33	188.00	0.89	7.72	1.4
8	4	-9	12.3	1790	5.1	62.33	14.00	58.33	10.67	63.67	2.21	19.22	3.1
9	4	-3	14.1	1642	11.1	42.38	28.43	48.87	24.93	36.40	1.92	16.70	3.7
10	4	-3	14.3	1526	11.1	45.41	14.88	46.42	17.83	37.50	0.00	0.00	4.0
11	8	-9	12.1	1797	5.8	46.78	15.83	57.17	1.00	57.67	2.92	25.13	3.1
12	8	-15	14.9	1790	2.0	55.98	43.29	73.25	69.50	108.00	1.01	8.79	2.4
13	8	-15	16.8	1790	2.5	43.83	33.75	58.00	50.00	83.00	1.20	10.38	3.1
14	8	-9	12.2	1907	5.8	55.62	23.40	67.33	23.33	79.00	2.53	21.93	2.6
15	8	-3	18.9	1429	9.7	51.04	26.43	60.67	16.00	52.67	1.61	13.99	2.9
16	12	-3	18.9	1487	9.4	44.44	19.33	51.17	12.33	45.00	0.00	0.00	3.6
17	12	-9	12.6	1874	4.3	53.49	17.43	63.83	7.67	67.67	2.78	24.15	2.8
18	12	-15	13.0	1773	2.1	43.89	35.00	57.58	57.83	86.50	0.60	5.19	3.1
19	12	-15	14.6	1761	0.4	83.66	91.11	116.60	166.80	200.00	0.00	0.00	1.4
20	12	-9	13.1	1799	6.0	56.25	11.63	63.00	6.00	66.00	2.43	21.08	2.8
21	16	-3	20.1	1494	10.5	45.64	13.54	49.33	10.67	44.00	0.00	0.00	3.7
22	16	-3	20.1	1621	8.2	42.75	12.38	49.13	11.25	54.75	2.94	25.52	3.7
23	16	-9	11.8	1854	5.1	50.82	14.43	59.33	6.67	62.67	2.73	23.66	3.0
24	16	-15	16.1	1720	1.1	91.40	90.56	127.17	147.67	201.00	1.02	8.84	1.3
25	16	-15	18.2	1760	0.6	32.60	25.63	42.35	43.96	64.33	0.00	0.00	4.4
26	20	-9	12.9	1904	5.6	55.61	26.92	69.08	26.83	82.50	2.59	22.46	2.5
27	20	-3	15.4	1515	9.7	44.42	24.88	50.63	20.75	40.25	2.17	18.44	3.6
28	20	-3	14.5	1694	8.5	33.44	21.66	31.30	24.60	43.60	3.22	27.98	6.2
29	20	-9	12.2	1897	5.5	51.17	19.42	63.00	6.67	66.33	2.44	21.19	2.8
30	20	-15	13.8	1837	1.9	44.40	34.60	58.70	52.60	85.00	0.79	6.82	3.1
31	24	-15	18.6	1692	1.9	94.08	54.13	116.75	80.50	157.00	0.00	0.00	1.4
32	24	-9	11.2	1906	7.2	53.78	15.83	61.17	19.00	70.67	3.10	26.87	2.9
33	24	-3	21.9	1422	10.2	60.26	44.28	81.67	48.67	106.00	0.00	0.00	2.1
34	24	-3	16.9	1499	9.7	46.89	18.33	57.17	11.67	63.00	0.00	0.00	3.1
35	24	-9	12.9	1938	5.9	71.44	12.83	80.00	0.00	80.00	2.81	24.37	2.2
36	28	-15	15.6	1795	2.4	105.22	48.67	129.50	49.00	154.00	1.44	12.45	1.3
37	28	-15	20.0	1727	1.8	58.44	33.83	73.50	45.00	96.00	0.00	0.00	2.4
38	28	-9	11.2	1917	5.2	72.78	30.33	83.50	19.00	74.00	2.50	21.66	2.1
39	28	-3	25.4	1334	6.8	41.81	22.29	49.71	13.92	42.75	1.51	13.13	3.7
40	28	-3	15.2	1543	9.3	36.55	24.18	43.50	18.27	34.40	2.21	19.22	4.3
41	32	-9	12.7	1885	4.9	58.97	31.80	71.75	50.50	97.00	2.04	17.73	2.4
42	32	-15	14.4	1734	1.0	38.33	22.50	48.50	29.00	63.00	0.00	0.00	3.8
43	32	-15	14.5	1825	0.7	52.06	15.58	59.33	18.67	68.67	0.00	0.00	3.0
44	32	-9	12.0	1900	5.4	67.14	29.13	80.58	35.83	98.50	2.61	22.64	2.1
45	32	-3	24.9	1429	6.5	50.52	33.46	65.00	47.00	88.50	2.10	18.25	2.7
46	36	-3	16.2	1581	10.2	40.41	20.38	47.70	12.60	41.40	2.00	17.36	3.8
47	36	-9	12.7	1850	3.8	62.75	21.38	74.50	15.00	82.00	2.84	24.62	2.3
48	36	-15	16.9	1816	2.2	80.57	63.14	107.50	91.00	153.00	0.00	0.00	1.5
49	36	-15	18.0	1771	2.3	86.02	63.30	111.33	101.33	162.00	1.02	10.76	1.5
50	36	-9	13.6	1824	4.4	63.40	29.40	78.50	27.00	92.00	2.70	23.39	2.2
51	40	-3	19.1	1377	7.4	40.12	33.32	47.27	30.13	32.20	0.00	0.00	3.9
		Average	15.3	1725	5.5	56.6	30.2	68.5	35.9	81.4	1.6	13.9	2.9
		Stdev	3.35	163.16	3.36	17.35	18.99	24.05	36.78	43.52	1.14	9.87	1.00

Project 4	Knapp Street Ames, IA
Date	5/21/2003

	Coordinates		Nuc Gage Results			450 mm		300 mm		150 mm	Geogage	
Test #	X	Y	% Moisture	Dry Density, kg/m^3	CIV	Mean DCP Index, mm/blow	Mean Change in DCP Index, mm/blow	Mean DCP Index, mm/blow	Mean Change in DCP Index, mm/blow	Mean DCP Index, mm/blow	Stiffness, MN/m	Modulus, kPa
1	0	-15	13.4	1716	2.4	86.06	20.67	94.75	30.50	110.00	1.36	11.79
2	0	-9	15.1	1765	7.5	49.22	11.17	54.71	3.92	52.75	3.06	26.58
3	0	-3	14.7	1723	10.9	39.93	28.60	43.00	32.00	27.00	3.16	27.44
4	0	-3	12.4	1724	10.9	37.11	26.83	41.58	26.83	28.17	2.52	21.90
5	0	-9	11.4	1942	4.9	52.84	16.07	62.17	8.33	66.33	2.22	19.24
6	4	-15	13.9	1819	2.2	73.08	25.88	87.75	15.50	95.50	2.15	18.65
7	4	-15	14.8	1858	1.2	87.13	82.64	119.33	137.33	188.00	0.89	7.72
8	4	-9	12.3	1790	5.1	62.33	14.00	58.33	10.67	63.67	2.21	19.22
9	4	-3	14.1	1642	11.1	42.38	28.43	48.87	24.93	36.40	1.92	16.70
10	4	-3	14.3	1526	11.1	45.41	14.88	46.42	17.83	37.50	0.00	0.00
11	8	-9	12.1	1797	5.8	46.78	15.83	57.17	1.00	57.67	2.92	25.13
12	8	-15	14.9	1790	2.0	55.98	43.29	73.25	69.50	108.00	1.01	8.79
13	8	-15	16.8	1790	2.5	43.83	33.75	58.00	50.00	83.00	1.20	10.38
14	8	-9	12.2	1907	5.8	55.62	23.40	67.33	23.33	79.00	2.53	21.93
15	8	-3	18.9	1429	9.7	51.04	26.43	60.67	16.00	52.67	1.61	13.99
16	12	-3	18.9	1487	9.4	44.44	19.33	51.17	12.33	45.00	0.00	0.00
17	12	-9	12.6	1874	4.3	53.49	17.43	63.83	7.67	67.67	2.78	24.15
18	12	-15	13.0	1773	2.1	43.89	35.00	57.58	57.83	86.50	0.60	5.19
19	12	-15	14.6	1761	0.4	83.66	91.11	116.60	166.80	200.00	0.00	0.00
20	12	-9	13.1	1799	6.0	56.25	11.63	63.00	6.00	66.00	2.43	21.08
21	16	-3	20.1	1494	10.5	45.64	13.54	49.33	10.67	44.00	0.00	0.00
22	16	-3	20.1	1621	8.2	42.75	12.38	49.13	11.25	54.75	2.94	25.52
23	16	-9	11.8	1854	5.1	50.82	14.43	59.33	6.67	62.67	2.73	23.66
24	16	-15	16.1	1720	1.1	91.40	90.56	127.17	147.67	201.00	1.02	8.84
25	16	-15	18.2	1760	0.6	32.60	25.63	42.35	43.96	64.33	0.00	0.00
26	20	-9	12.9	1904	5.6	55.61	26.92	69.08	26.83	82.50	2.59	22.46
27	20	-3	15.4	1515	9.7	44.42	24.88	50.63	20.75	40.25	2.17	18.44
28	20	-3	14.5	1694	8.5	33.44	21.66	31.30	24.60	43.60	3.22	27.98
29	20	-9	12.2	1897	5.5	51.17	19.42	63.00	6.67	66.33	2.44	21.19
30	20	-15	13.8	1837	1.9	44.40	34.60	58.70	52.60	85.00	0.79	6.82
31	24	-15	18.6	1692	1.9	94.08	54.13	116.75	80.50	157.00	0.00	0.00
32	24	-9	11.2	1906	7.2	53.78	15.83	61.17	19.00	70.67	3.10	26.87
33	24	-3	21.9	1422	10.2	60.26	44.28	81.67	48.67	106.00	0.00	0.00
34	24	-3	16.9	1499	9.7	46.89	18.33	57.17	11.67	63.00	0.00	0.00
35	24	-9	12.9	1938	5.9	71.44	12.83	80.00	0.00	80.00	2.81	24.37
36	28	-15	15.6	1795	2.4	105.22	48.67	129.50	49.00	154.00	1.44	12.45
37	28	-15	20.0	1727	1.8	58.44	33.83	73.50	45.00	96.00	0.00	0.00
38	28	-9	11.2	1917	5.2	72.78	30.33	83.50	19.00	74.00	2.50	21.66
39	28	-3	25.4	1334	6.8	41.81	22.29	49.71	13.92	42.75	1.51	13.13
40	28	-3	15.2	1543	9.3	36.55	24.18	43.50	18.27	34.40	2.21	19.22
41	32	-9	12.7	1885	4.9	58.97	31.80	71.75	50.50	97.00	2.04	17.73
42	32	-15	14.4	1734	1.0	38.33	22.50	48.50	29.00	63.00	0.00	0.00
43	32	-15	14.5	1825	0.7	52.06	15.58	59.33	18.67	68.67	0.00	0.00
44	32	-9	12.0	1900	5.4	67.14	29.13	80.58	35.83	98.50	2.61	22.64
45	32	-3	24.9	1429	6.5	50.52	33.46	65.00	47.00	88.50	2.10	18.25
46	36	-3	16.2	1581	10.2	40.41	20.38	47.70	12.60	41.40	2.00	17.36
47	36	-9	12.7	1850	3.8	62.75	21.38	74.50	15.00	82.00	2.84	24.62
48	36	-15	16.9	1816	2.2	80.57	63.14	107.50	91.00	153.00	0.00	0.00
49	36	-15	18.0	1771	2.3	86.02	63.30	111.33	101.33	162.00	1.02	10.76
50	36	-9	13.6	1824	4.4	63.40	29.40	78.50	27.00	92.00	2.70	23.39
51	40	-3	19.1	1377	7.4	40.12	33.32	47.27	30.13	32.20	0.00	0.00
		Average	15.3	1725.0	5.5	56.6	30.2	68.5	35.9	81.4	1.6	13.9
		Stdev	3.35	163.16	3.36	17.35	18.99	24.05	36.78	43.52	1.14	9.87

Project 5	35th St. and I-235 WB Ramp NW QUAD
Date	5/21/2003

	Coordinates		Nuc Gage Results			450 mm		300 mm		150 mm	Geogage	
Test #	X	Y	% Moisture	Dry Density, kg/m^3	CIV	Mean DCP Index, mm/blow	Mean Change in DCP Index, mm/blow	Mean DCP Index, mm/blow	Mean Change in DCP Index, mm/blow	Mean DCP Index, mm/blow	Stiffness, MN/m	Modulus, kPa
1	0	-8	12.6	1927	9.8	35.40	3.90	36.40	3.20	34.80	5.96	51.67
2	0	-4	14.7	1805	3.1	41.82	15.93	47.83	27.67	61.67	4.91	42.61
3	0	0	16.0	1772	5.7	34.99	15.33	40.31	29.38	55.00	5.32	46.14
4	0	4	14.2	1793	6.3	25.35	9.33	29.36	13.29	36.00	4.79	41.54
5	0	8	13.7	1863	5.5	33.54	13.86	38.67	24.67	51.00	4.48	38.87
6	4	8	12.0	1813	5.3	27.33	11.18	32.05	16.39	40.25	3.62	31.39
7	4	4	12.6	1911	11.3	29.94	13.50	36.17	16.67	44.50	5.38	46.70
8	4	0	13.3	1850	4.7	37.56	17.58	42.08	32.50	58.33	5.48	47.57
9	4	-4	10.4	1920	4.0	35.28	19.42	42.67	33.33	59.33	4.97	43.15
10	4	-8	13.8	1874	8.6	33.99	14.27	37.65	11.70	31.80	7.12	61.73
11	8	-8	11.0	1856	8.4	33.11	17.08	35.33	18.33	26.17	5.17	44.83
12	8	-4	14.5	1810	3.6	37.45	17.43	45.10	23.80	57.00	4.97	43.08
13	8	0	12.2	1891	5.8	32.36	15.06	38.73	22.04	49.75	4.67	40.49
14	8	4	11.9	1894	6.8	32.27	17.85	39.10	30.48	54.33	6.39	55.40
15	8	8	12.9	1903	7.6	31.44	9.02	31.46	12.07	37.50	4.29	37.19
16	12	8	11.1	1893	7.8	32.02	4.03	34.37	2.07	35.40	4.51	39.16
17	12	4	11.6	1882	13.3	36.10	12.25	40.90	20.20	51.00	6.24	54.13
18	12	0	12.4	1860	4.4	39.16	19.33	46.73	31.87	62.67	3.48	30.17
19	12	-4	12.6	1848	4.2	54.93	24.85	65.50	36.00	83.50	4.96	43.05
20	12	-8	11.0	1885	8.9	36.44	9.83	40.00	6.00	37.00	3.43	29.74
21	16	-8	10.9	1939	7.0	34.29	14.19	39.58	8.35	35.40	3.75	32.55
22	16	-4	13.1	1839	3.7	53.50	33.75	66.75	55.50	94.50	4.50	39.02
23	16	0	13.3	1838	3.1	46.78	29.44	57.35	54.30	84.50	4.08	35.42
24	16	4	15.3	1852	5.6	37.35	17.07	44.10	27.80	58.00	5.00	43.39
25	16	8	12.9	1853	6.1	33.57	10.20	38.43	11.65	44.25	4.48	38.88
26	20	8	14.1	1826	4.4	34.93	12.58	39.81	21.05	50.33	3.87	33.54
27	20	4	13.6	1879	3.9	32.60	20.18	41.25	28.83	55.67	5.11	44.31
28	20	0	13.1	1907	9.0	23.47	10.29	29.00	8.00	33.00	5.67	49.15

29	20	-4	15.5	1794	4.7	48.17	20.75	55.25	40.50	75.50	5.62	48.74
30	20	-8	11.6	1906	6.7	33.69	16.58	36.88	15.75	29.00	3.79	32.84
31	24	-8	10.2	1933	8.6	31.61	14.08	33.08	15.83	25.17	6.19	53.70
32	24	-4	10.9	1863	12.0	32.06	8.51	36.80	5.60	39.60	4.77	41.39
33	24	0	11.5	1883	9.2	35.67	12.17	39.83	23.67	51.67	3.75	32.51
34	24	4	12.9	1879	5.1	29.21	12.19	34.38	17.75	43.25	5.14	44.57
35	24	8	14.4	1826	4.6	32.36	15.21	38.65	7.70	34.80	4.09	35.48
36	28	8	13.0	1891	6.1	28.58	4.62	29.45	7.90	33.40	4.32	37.44
37	28	4	12.7	1894	5.2	32.65	11.22	38.70	8.60	43.00	5.38	46.64
38	28	0	13.0	1909	7.2	34.86	16.04	42.67	17.33	51.33	6.16	53.48
39	28	-4	11.2	1942	3.3	39.60	5.48	43.00	0.50	42.75	5.50	47.73
40	28	-8	13.8	1811	9.2	42.02	9.10	38.53	15.45	30.80	4.95	42.92
41	32	-8	10.0	1891	6.9	30.83	20.13	30.85	26.81	17.44	2.72	23.61
42	32	-4	10.5	1892	3.3	61.28	28.17	66.25	47.50	90.00	2.47	21.40
43	32	0	11.7	1920	7.2	35.14	13.71	34.38	16.75	42.75	6.24	54.14
44	32	4	12.4	1890	7.5	24.58	12.04	28.79	22.92	40.25	4.90	42.55
45	32	8	14.3	1851	6.3	26.49	7.55	30.68	5.03	32.20	4.23	36.68
46	36	8	11.9	1903	4.7	29.33	12.50	34.00	22.00	45.00	3.77	32.75
47	36	4	12.9	1891	6.3	32.12	16.42	39.85	19.30	49.50	4.57	39.60
48	36	0	11.3	1892	8.7	27.44	9.33	32.00	10.00	37.00	4.37	37.89
49	36	-4	10.9	1895	3.5	44.30	34.65	58.10	55.80	86.00	3.75	32.53
50	36	-8	10.6	1905	8.8	29.31	7.93	29.80	9.60	25.00	6.37	55.25
51	40	-8	12.2	1907	7.2	33.33	3.40	34.50	2.20	33.40	2.71	23.48
52	40	-4	15.3	1803	3.1	51.71	35.43	66.00	56.00	94.00	4.28	37.15
53	40	0	15.5	1794	3.8	44.08	29.69	55.55	49.90	80.50	3.30	28.65
54	40	4	14.5	1826	4.7	35.11	13.67	39.50	27.00	53.00	4.96	43.04
55	40	8	14.1	1876	4.5	36.31	17.79	42.75	32.50	59.00	3.66	31.73
56	44	8	12.5	1862	4.3	38.59	11.45	44.17	12.33	50.33	3.10	26.93
57	44	4	11.7	1885	7.5	24.56	7.58	23.08	7.17	26.67	4.69	40.73
58	44	0	14.4	1807	4.4	34.86	18.22	37.19	28.95	51.67	3.74	32.44
59	44	-4	12.4	1879	4.3	55.19	36.08	69.13	60.75	99.50	3.54	30.67
60	44	-8	12.9	1889	6.6	35.23	13.90	37.65	13.70	30.80	5.92	51.35
61	48	-8	10.9	1912	8.5	32.36	17.46	34.79	18.43	25.57	4.62	40.11
62	48	-4	12.8	1870	2.8	40.58	15.00	32.66	18.18	23.57	4.17	36.20
63	48	0	12.8	1848	6.6	31.04	10.99	32.23	17.04	40.75	4.28	37.14
64	48	4	13.7	1888	8.3	24.41	4.92	24.40	6.54	27.67	5.65	49.00
65	48	8	10.4	1944	8.2	25.89	6.11	28.04	11.51	33.80	3.95	34.36

66	52	8	13.8	1891	7.3	27.49	6.58	31.12	4.57	33.40	5.68	49.25
67	52	4	11.6	1940	7.9	27.97	6.35	31.20	2.00	30.20	5.90	51.14
68	52	0	13.3	1849	5.9	31.08	6.96	33.71	12.08	39.75	5.28	45.81
69	52	-4	12.2	1841	5.8	38.33	15.17	44.83	21.67	55.67	3.37	29.22
70	52	-8	11.2	1845	8.8	34.30	8.43	30.95	13.61	24.14	3.94	34.15
71	56	-8	11.5	1865	8.7	38.48	5.15	35.48	2.55	34.20	6.34	54.98
72	56	-4	13.1	1885	2.8	41.06	16.24	49.17	16.33	57.33	2.78	24.16
73	56	0	12.7	1888	3.8	36.52	16.79	39.00	27.33	52.67	4.40	38.18
74	56	4	14.8	1904	5.8	29.25	9.04	33.17	12.67	39.50	5.43	47.13
75	56	8	13.7	1852	5.7	36.22	13.75	41.08	25.83	54.00	4.52	39.18
76	60	8	11.5	1941	4.3	38.17	19.75	42.50	35.00	60.00	4.37	37.94
77	60	4	13.7	1881	4.2	29.76	7.00	31.50	13.00	38.00	3.84	33.35
78	60	0	13.3	1884	3.4	36.46	16.43	39.58	28.17	53.67	5.12	44.42
79	60	-4	12.7	1862	3.8	36.14	19.07	40.71	34.57	58.00	4.08	35.36
80	60	-8	10.1	1940	6.6	38.23	21.40	42.25	20.50	32.00	6.22	53.95
81	64	-8	12.0	1918	10.1	34.30	11.55	33.75	16.50	25.50	4.61	40.01
82	64	-4	13.3	1810	3.0	47.78	26.83	57.75	47.50	81.50	3.48	30.19
83	64	0	15.4	1811	4.5	32.89	10.58	35.42	19.17	45.00	4.27	37.00
84	64	4	11.9	1888	6.4	35.70	7.35	38.15	14.70	45.50	4.27	37.06
85	64	8	12.6	1880	4.8	37.67	17.50	43.33	34.67	60.67	4.08	35.41
86	68	8	16.6	1880	6.7	28.20	8.65	28.71	12.57	35.00	4.44	38.50
87	68	4	13.3	1923	6.4	25.13	6.19	26.00	10.00	31.00	4.33	37.54
88	68	0	12.1	1810	6.3	32.83	9.50	34.25	15.50	42.00	4.46	38.73
89	68	-4	20.3	1682	6.8	38.33	18.50	44.83	35.00	62.33	5.60	48.55
90	68	-8	10.8	1843	8.2	36.65	6.15	33.73	7.05	30.20	4.81	41.70
91	72	-8	10.1	1798	8.4	36.10	12.23	33.77	20.96	23.29	3.78	32.77
92	72	-4	15.3	1813	8.3	34.98	13.67	40.47	21.73	51.33	4.24	36.76
93	72	0	13.2	1874	5.3	26.56	4.49	27.99	8.83	32.40	4.62	40.09
94	72	4	13.6	1891	6.1	26.12	7.04	26.61	10.37	31.80	5.58	48.40
95	72	8	11.7	1896	6.7	24.97	13.00	24.95	17.30	33.60	4.94	42.83
96	76	8	11.9	1927	6.6	30.75	18.13	31.96	26.58	45.25	4.70	40.81
97	76	4	13.8	1896	5.7	26.98	7.47	27.80	11.60	33.60	6.57	39.62
98	76	0	14.6	1833	5.6	31.18	11.13	35.79	16.92	44.25	5.37	46.55
99	76	-4	16.1	1729	3.5	38.14	13.08	42.80	24.40	55.00	3.43	29.75
100	76	-8	12.7	1846	9.7	34.53	10.30	35.70	11.40	30.00	5.83	50.52
101	80	-8	13.1	1838	6.8	40.28	9.70	44.63	4.25	42.50	6.82	59.20
102	80	-4	14.3	1865	6.7	29.49	11.80	33.31	23.38	45.00	5.33	46.22

103	80	0	15.3	1835	4.1	33.10	16.43	37.57	30.86	53.00	4.36	37.86
104	80	4	16.6	1817	5.3	28.92	17.13	29.88	24.75	42.25	4.84	41.97
105	80	8	11.6	1856	4.2	38.96	26.61	44.28	46.11	67.33	3.53	30.62
106	84	8	11.2	1846	4.1	28.72	16.42	31.51	27.47	45.25	3.31	28.76
107	84	4	13.8	1856	5.8	27.70	12.15	29.05	18.90	38.50	5.27	45.68
108	84	0	15.7	1860	5.7	28.20	13.13	30.22	21.56	41.00	5.56	48.26
109	84	-4	16.5	1779	4.6	40.00	12.42	46.08	13.17	52.67	4.92	42.69
110	84	-8	10.6	1854	8.2	32.70	18.45	35.21	19.57	25.43	6.53	56.62
111	88	-8	8.5	1970	7.5	41.25	22.50	43.13	26.25	30.00	5.72	49.59
112	88	-4	13.3	1910	8.7	28.48	4.34	30.37	6.07	33.40	4.53	39.32
113	88	0	13.6	1917	7.5	26.13	6.56	26.98	10.45	32.20	4.83	41.94
114	88	4	15.3	1841	7.4	17.64	6.74	28.67	11.06	34.20	4.44	38.53
115	88	8	11.5	1929	4.8	35.63	6.15	37.85	11.30	43.50	4.04	35.03
116	92	8	14.4	1894	6.2	29.97	13.38	34.96	23.58	46.75	5.72	49.61
117	92	4	12.3	1920	6.3	23.75	11.31	26.24	10.09	21.20	6.24	54.21
118	92	0	11.8	1926	7.3	23.78	6.33	27.00	6.00	30.00	5.10	44.25
119	92	-4	16.5	1815	5.7	29.29	8.14	33.08	9.83	38.00	5.09	44.17
120	92	-8	9.3	1886	7.6	43.07	19.40	45.60	20.80	35.20	6.72	58.32
121	96	-8	11.8	1862	6.2	46.93	8.10	44.57	15.53	36.80	4.59	39.84
122	96	-4	12.3	1834	5.5	35.56	18.83	42.83	31.67	58.67	4.11	35.67
123	96	0	12.4	1867	7.8	30.19	6.03	29.58	6.83	33.00	4.01	38.81
124	96	4	12.4	1916	5.4	25.23	3.99	26.20	7.26	29.83	4.08	41.63
125	96	8	12.7	1922	6.7	28.93	8.10	32.90	8.60	37.20	5.04	43.71
126	100	8	12.7	1867	3.9	28.19	14.96	31.86	27.28	45.50	3.75	32.49
127	100	4	11.4	1839	6.2	29.46	10.76	34.58	12.35	40.75	4.12	35.76
128	100	0	13.0	1882	6.1	34.39	11.92	38.83	21.00	49.83	4.17	36.15
129	100	-4	12.7	1750	4.0	29.58	17.38	38.38	16.75	46.75	4.91	42.61
130	100	-8	12.1	1799	7.6	51.80	39.30	62.00	32.00	46.00	5.33	46.28
		average	12.9	1867.7	6.2	34.2	13.8	38.1	20.0	44.9	4.7	40.9
		Stdev	1.75	46.89	2.01	7.17	7.14	9.26	12.66	16.30	0.95	8.08
		Hi	20.3	1942	13.3	61.28	36.08	69.13	60.75	99.5	7.12	61.73
		Low	8.5	1772	2.8	23.47	3.4	23.08	0.5	21.2	2.47	21.4

Project 6	35th St. and I-235 WB Ramp (SUBBASE)
Date	6/13/2003

	Coordinates		Nuc Gauge Results			600 mm		300 mm	Geogage	
Test #	X	Y	% Moisture	Dry Density, kg/m^3	CIV	Mean DCP Index, mm/blow	Mean Change in DCP Index, mm/blow	Mean DCP Index, mm/blow	Stiffness, MN/m	Modulus, kPa
1	0	0	11.1	1676	16.0	---	---	---	5.45	47.28
2	-10	0	7.4	1823	28.7	---	---	---	7.09	61.53
3	-20	0	7.5	1764	22.6	---	---	---	7.91	68.58
4	-30	0	7.4	1823	24.3	---	---	---	7.79	67.56
5	-40	0	9.6	1768	23.3	---	---	---	4.15	36.03
6	-50	0	7.4	1747	22.9	---	---	---	7.80	67.66
7	-50	10	8.1	1938	28.7	---	---	---	4.20	36.40
8	-40	10	10.5	1658	13.2	---	---	---	4.36	37.79
9	-30	10	10.6	1737	11.7	---	---	---	5.47	47.48
10	-20	10	7.4	2006	16.6	---	---	---	5.56	48.27
11	-10	10	7.9	1726	18.6	---	---	---	4.93	42.81
12	0	10	9.5	1918	22.2	---	---	---	6.94	60.21
13	0	20	9.0	1881	19.5	---	---	---	4.94	42.82
14	-10	20	7.6	1816	27.0	---	---	---	9.65	83.70
15	-20	20	7.5	1892	27.0	---	---	---	7.81	67.76
16	-30	20	8.3	1680	10.9	---	---	---	4.65	40.34
17	-40	20	11.6	1517	11.4	---	---	---	4.55	39.46
18	-50	20	7.8	1899	14.5	---	---	---	3.51	30.41
19	-50	30	8.6	1819	24.5	---	---	---	2.36	20.50
20	-40	30	9.5	1844	23.6	---	---	---	5.92	51.38
21	-30	30	8.5	1946	21.5	---	---	---	5.25	45.51
22	-20	30	7.2	1734	26.5	---	---	---	8.80	76.30
23	-10	30	6.8	2026	25.3	---	---	---	5.66	49.10
24	0	30	8.0	1915	15.9	---	---	---	6.30	54.68
		Average	8.5	1814.7	20.7	---	---	---	5.9	51.0
		Stdev	1.35	120.37	5.68	---	---	---	1.78	15.43

Project 7	Hwy. 34 EBL East of Fairfield
Date	7/2/2003

	Coordinates		Nuc Gage Results			450 mm		300 mm		150 mm	Geogage	
Test #	X	Y	% Moisture	Dry Density, kg/m^3	CIV	Mean DCP Index, mm/blow	Mean Change in DCP Index, mm/blow	Mean DCP Index, mm/blow	Mean Change in DCP Index, mm/blow	Mean DCP Index, mm/blow	Stiffness, MN/m	Modulus, kPa
1	0	-12	10.6	1970	11.7	20.76	3.36	19.85	6.30	16.70	6.51	56.46
2	0	-6	7.5	2086	10.4	28.89	4.54	26.94	6.45	23.71	5.59	48.52
3	0	0	6.4	1938	8.0	32.20	2.40	33.30	1.00	32.80	4.48	38.86
4	0	6	7.4	1966	12.2	25.25	4.24	24.30	3.74	26.17	6.14	53.25
5	0	12	5.8	2037	13.0	33.39	25.92	33.48	34.37	16.30	9.22	79.98
6	4	12	6.9	2052	10.7	28.46	9.81	25.89	18.22	16.78	8.94	77.53
7	4	6	6.3	2016	8.9	32.00	2.10	32.20	3.20	33.80	5.08	44.10
8	4	0	6.2	1844	6.7	31.85	14.56	30.57	16.86	39.00	4.80	41.67
9	4	-6	6.8	2084	12.1	32.71	9.44	29.56	18.88	20.13	5.99	51.94
10	4	-12	7.1	2045	11.5	26.18	5.12	26.44	6.31	23.29	6.95	60.31
11	8	-12	6.7	2126	11.6	21.56	12.96	24.54	11.31	18.89	8.36	72.49
12	8	-6	6.1	2103	12.2	26.35	5.06	24.52	9.29	19.88	7.04	61.06
13	8	0	5.6	1908	8.0	22.22	9.91	26.03	16.73	34.40	3.96	34.33
14	8	6	6.5	1973	10.5	28.42	5.37	29.42	5.17	26.83	5.04	43.70
15	8	12	6.7	1981	11.7	27.01	5.42	25.10	10.20	20.00	4.80	41.66
16	12	12	6.7	2026	10.8	27.58	11.13	25.45	19.10	15.90	5.06	43.88
17	12	6	6.2	2016	8.5	28.76	4.56	31.57	0.47	31.33	6.40	55.52
18	12	0	5.8	1926	7.2	32.52	7.88	37.28	2.95	38.75	4.74	41.10
19	12	-6	6.5	2005	11.0	37.32	7.27	28.23	7.88	24.29	4.52	39.24
20	12	-12	7.4	2041	14.0	23.59	6.70	21.13	12.07	15.10	8.01	69.50
21	16	-12	7.6	2056	15.5	22.19	6.23	19.21	7.01	15.70	7.70	66.80
22	16	-6	6.9	2055	10.2	26.50	5.55	26.67	7.06	23.14	5.85	50.78
23	16	0	7.0	1967	8.7	29.81	8.29	34.00	8.00	38.00	6.94	60.22
24	16	6	7.4	2040	8.2	27.08	4.98	27.70	5.40	25.00	4.67	40.53
25	16	12	7.0	2009	8.4	27.26	4.89	24.29	0.57	24.57	6.09	52.85
26	20	12	6.5	2067	12.0	---	---	---	---	25.67	4.83	41.89
27	20	6	6.9	2061	8.4	---	---	---	---	30.17	4.71	40.82
28	20	0	6.2	1937	9.3	---	---	---	---	29.17	6.57	56.98

29	20	-6	7.3	2071	11.5	---	---	---	---	22.86	5.51	47.83
30	20	-12	6.9	2129	12.2	---	---	---	---	15.73	7.66	66.48
31	24	-12	7.4	1981	12.1	---	---	---	---	21.43	8.58	74.42
32	24	-6	6.4	2123	9.6	---	---	---	---	22.29	5.90	51.21
33	24	0	6.3	2076	9.3	---	---	---	---	24.29	5.06	43.87
34	24	6	6.2	2092	9.9	---	---	---	---	30.00	5.05	43.80
35	24	12	6.4	2081	11.9	---	---	---	---	23.43	5.75	49.84
36	28	12	6.2	2058	10.9	---	---	---	---	23.13	6.19	53.71
37	28	6	7.3	1945	9.8	---	---	---	---	31.60	5.36	46.48
38	28	0	6.5	1949	9.5	---	---	---	---	24.14	5.05	43.81
39	28	-6	7.3	2049	8.5	---	---	---	---	27.50	5.66	49.14
40	28	-12	7.4	2086	12.7	---	---	---	---	18.67	7.56	65.61
41	32	-12	7.4	2073	10.6	---	---	---	---	19.75	6.19	53.73
42	32	-6	8.1	2077	8.8	---	---	---	---	29.67	4.17	36.21
43	32	0	7.6	2057	8.2	---	---	---	---	43.75	4.19	36.34
44	32	6	7.5	2051	8.4	---	---	---	---	23.86	6.18	53.57
45	32	12	5.4	2073	14.0	---	---	---	---	22.57	8.24	71.45
46	36	12	6.0	2045	11.6	---	---	---	---	18.44	5.89	51.08
47	36	6	7.2	2032	10.0	---	---	---	---	23.00	5.49	47.03
48	36	0	7.9	1953	9.8	---	---	---	---	28.67	5.69	49.35
49	36	-6	8.8	1976	9.2	---	---	---	---	30.17	4.45	38.64
50	36	-12	6.5	2095	13.7	---	---	---	---	25.00	5.10	44.24
51	40	-12	6.9	2087	11.6	---	---	---	---	18.33	7.35	63.75
52	40	-6	8.0	1946	9.7	---	---	---	---	30.40	4.97	43.11
53	40	0	6.0	2007	8.2	---	---	---	---	17.00	4.47	38.76
54	40	6	6.5	2066	10.3	---	---	---	---	24.57	6.14	53.28
55	40	12	5.7	2061	13.9	---	---	---	---	17.89	5.41	46.91
56	44	12	7.4	1983	10.0	---	---	---	---	21.00	6.20	53.79
57	44	6	8.0	2091	11.3	---	---	---	---	19.78	6.26	54.33
58	44	0	8.1	2001	9.3	---	---	---	---	28.67	4.93	42.75
59	44	-6	7.7	2050	9.9	---	---	---	---	21.71	4.82	41.82
60	44	-12	6.8	2108	10.4	---	---	---	---	21.00	7.41	64.31
61	48	-12	7.2	2010	10.8	---	---	---	---	26.00	6.01	52.12
62	48	-6	8.1	2045	9.8	---	---	---	---	30.20	5.30	46.02
63	48	0	7.2	1971	11.2	---	---	---	---	27.83	6.46	56.02
64	48	6	6.4	2058	11.3	---	---	---	---	20.67	8.21	71.23
65	48	12	6.3	2052	10.1	---	---	---	---	18.88	4.68	40.62
66	52	12	6.3	2009	10.8	---	---	---	---	17.89	4.98	43.22
67	52	6	7.3	2037	11.0	---	---	---	---	23.57	5.91	51.26
68	52	0	8.4	2053	10.7	---	---	---	---	22.86	4.51	39.10
69	52	-6	6.8	2063	8.6	---	---	---	---	25.00	4.02	34.89
70	52	-12	8.8	2007	10.0	---	---	---	---	25.50	6.88	59.68
71	56	-12	8.3	2045	8.4	---	---	---	---	42.00	5.57	48.32
72	56	-6	7.5	1979	10.0	---	---	---	---	31.50	5.05	43.82
73	56	0	8.0	2019	10.7	---	---	---	---	25.17	4.91	42.63
74	56	6	6.9	2046	11.7	---	---	---	---	24.43	6.67	57.85
75	56	12	6.7	2056	10.9	---	---	---	---	21.71	6.26	54.35
76	60	12	6.7	2018	11.7	---	---	---	---	21.43	6.22	53.94
77	60	6	6.9	1995	7.7	---	---	---	---	29.83	4.68	40.62
78	60	0	7.5	2019	9.6	---	---	---	---	26.33	4.49	38.99
79	60	-6	7.6	1998	11.1	---	---	---	---	30.00	4.89	42.45
80	60	-12	11.2	1926	8.8	---	---	---	---	39.80	5.51	47.77
81	64	-12	8.3	1960	9.2	---	---	---	---	30.00	5.00	43.38
82	64	-6	8.2	2022	10.1	---	---	---	---	30.00	4.51	39.14
83	64	0	7.4	2068	9.9	---	---	---	---	24.43	6.37	55.25
84	64	6	8.2	2043	9.1	---	---	---	---	33.40	4.72	40.94
85	64	12	6.7	2082	10.8	---	---	---	---	20.00	6.05	52.50
		Average	7.1	2028.1	10.4	27.99	7.51	27.51	9.54	25.23	5.81	50.39
		Stdev	0.96	54.72	1.67	4.14	4.95	4.50	7.70	6.35	1.21	10.47

Project 8	Hwy. 218 SBL South of Mt. Pleasant
Date	7/1/2003

	Coordinates		Nuc Gage Results			450 mm		300 mm		150 mm	Geogage	
Test #	X	Y	% Moisture	Dry Density, kg/m^3	CIV	Mean DCP Index, mm/blow	Mean Change in DCP Index, mm/blow	Mean DCP Index, mm/blow	Mean Change in DCP Index, mm/blow	Mean DCP Index, mm/blow	Stiffness, MN/m	Modulus, kPa
1	0	-12	7.2	1974	39.4	17.22	8.29	13.99	13.80	7.09	5.26	45.67
2	0	-6	7.1	1993	23.8	20.87	13.04	12.55	2.24	11.43	8.23	71.36
3	0	0	7.1	1966	26.0	10.33	6.50	8.00	4.00	10.00	6.99	60.67
4	0	6	8.0	1964	28.4	13.93	2.91	12.45	2.76	11.07	11.35	98.46
5	0	12	9.7	1885	16.0	31.93	9.83	26.77	2.79	28.17	6.23	54.03
6	4	12	9.0	1875	24.0	---	---	---	---	12.08	8.22	71.30
7	4	6	7.5	1976	26.4	---	---	---	---		8.40	72.87
8	4	0	8.8	1972	26.0	---	---	---	---	8.33	13.29	115.31
9	4	-6	8.0	1946	24.6	---	---	---	---		8.68	75.30
10	4	-12	6.8	2028	29.4	---	---	---	---	9.75	4.80	41.64
11	8	-12	6.8	2101	30.9	---	---	---	---		5.75	49.87
12	8	-6	8.1	2019	21.4	---	---	---	---		4.70	70.81
13	8	0	7.1	2001	27.6	---	---	---	---		7.64	66.30
14	8	6	8.2	2012	33.4	---	---	---	---		9.15	79.38
15	8	12	8.0	1913	19.7	---	---	---	---		7.44	64.54
16	12	12	8.0	2002	27.5	---	---	---	---	13.73	6.78	58.82
17	12	6	6.7	1986	40.3	---	---	---	---		7.01	60.85
18	12	0	7.7	2079	31.1	---	---	---	---	11.85	6.04	52.36
19	12	-6	8.2	1984	17.7	---	---	---	---		9.05	78.52
20	12	-12	8.4	1913	24.3	---	---	---	---	8.61	10.23	88.71
21	16	-12	8.9	1948	31.3	---	---	---	---		8.91	77.27
22	16	-6	9.9	1925	27.8	---	---	---	---		9.01	78.16
23	16	0	9.1	1995	27.6	---	---	---	---		5.75	49.85
24	16	6	7.9	2086	39.3	---	---	---	---		5.77	50.09
25	16	12	8.3	1952	26.7	---	---	---	---		8.14	70.63
26	20	12	9.2	1930	15.3	---	---	---	---	16.78	6.94	60.23
27	20	6	6.9	2051	21.5	---	---	---	---		5.67	49.23
28	20	0	5.7	1935	39.1	---	---	---	---	6.25	3.95	34.30

29	20	-6	7.1	1964	29.7	---	---	---	---		6.91	59.96
30	20	-12	7.3	2000	22.6	---	---	---	---	13.08	9.70	84.11
31	24	-12	7.8	1858	15.3	---	---	---	---		7.82	67.86
32	24	-6	7.1	1943	31.4	---	---	---	---		7.88	68.32
33	24	0	6.8	2043	23.5	---	---	---	---		6.93	60.12
34	24	6	7.0	1992	24.1	---	---	---	---		8.52	73.94
35	24	12	7.2	1961	27.8	---	---	---	---		9.89	85.77
36	28	12	7.2	1939	34.8	---	---	---	---	15.10	5.85	50.51
37	28	6	10.5	1992	27.9	---	---	---	---		7.43	64.47
38	28	0	6.8	2046	26.4	---	---	---	---	7.50	7.34	63.70
39	28	-6	8.8	1976	18.3	---	---	---	---		4.99	43.26
40	28	-12	7.3	2003	27.3	---	---	---	---	11.33	9.14	79.32
41	32	-12	6.2	2044	32.0	---	---	---	---		7.86	68.17
42	32	-6	7.7	2029	20.2	---	---	---	---		6.28	54.47
43	32	0	6.7	2034	36.7	---	---	---	---		5.18	44.98
44	32	6	7.0	1971	37.5	---	---	---	---		4.66	40.40
45	32	12	7.5	1938	30.8	---	---	---	---		9.46	82.07
46	36	12	7.0	1932	23.5	---	---	---	---	14.00	10.90	94.58
47	36	6	9.9	1947	28.6	---	---	---	---		6.06	52.56
48	36	0	6.7	2064	34.8	---	---	---	---	7.50	3.12	27.05
49	36	-6	6.4	2055	30.2	---	---	---	---		1.86	16.13
50	36	-12	9.7	1954	28.1	---	---	---	---	12.75	6.81	59.07
51	40	-12	7.1	2030	34.5	---	---	---	---		8.88	77.01
52	40	-6	7.4	2007	21.3	---	---	---	---		4.06	35.25
53	40	0	6.6	2080	32.0	---	---	---	---		9.24	80.14
54	40	6	8.2	2067	35.4	---	---	---	---		8.52	73.89
55	40	12	6.3	1973	22.2	---	---	---	---		9.50	82.41
56	44	12	8.2	1940	15.4	---	---	---	---		5.01	43.49
57	44	6	11.3	1834	32.7	---	---	---	---		6.09	52.80
58	44	0	7.0	1964	38.5	---	---	---	---		2.35	20.37
59	44	-6	7.9	1995	31.4	---	---	---	---		6.97	60.50
60	44	-12	6.5	2138	27.9	---	---	---	---		6.98	60.56
61	48	-12	7.6	2009	19.0	---	---	---	---		6.72	58.27
62	48	-6	7.4	1997	22.6	---	---	---	---		7.09	61.47
63	48	0	6.9	1997	30.0	---	---	---	---		7.14	61.98
64	48	6	7.8	2060	28.2	---	---	---	---		7.38	64.03
65	48	12	6.5	1963	23.4	---	---	---	---		8.03	69.62
66	52	12	7.2	2010	28.2	---	---	---	---		12.01	104.14
67	52	6	7.0	2068	48.1	---	---	---	---		4.07	35.28
68	52	0	8.1	1988	29.4	---	---	---	---		6.46	56.03
69	52	-6	7.5	1909	29.3	---	---	---	---		7.40	64.18
70	52	-12	7.0	1973	11.4	---	---	---	---		6.22	53.97
71	56	-12	8.0	1982	22.3	---	---	---	---		6.59	57.15
72	56	-6	8.2	2041	33.6	---	---	---	---		7.89	68.41
73	56	0	7.2	2061	32.1	---	---	---	---		6.19	53.66
74	56	6	6.9	2031	39.2	---	---	---	---		10.46	90.72
75	56	12	6.8	2028	16.0	---	---	---	---		7.70	66.97
76	60	12	6.6	2017	18.8	---	---	---	---		11.34	98.41
77	60	6	6.4	1994	37.8	---	---	---	---		6.82	59.13
78	60	0	5.7	2042	23.6	---	---	---	---		4.45	38.60
79	60	-6	8.0	2016	19.6	---	---	---	---		6.18	56.65
80	60	-12	7.4	2050	27.1	---	---	---	---		9.18	79.63
81	64	-12	7.9	1957	24.9	---	---	---	---		6.62	57.46
82	64	-6	8.3	2017	12.5	---	---	---	---		7.48	64.86
83	64	0	6.9	2026	22.5	---	---	---	---		5.90	51.16
84	64	6	5.5	1939	23.6	---	---	---	---		6.64	57.62
85	64	12	5.9	1885	22.6	---	---	---	---		5.99	52.01
		Average	7.6	1990.4	27.2	18.9	8.1	14.8	5.1	11.8	7.22	63.00
		Stdev	1.07	56.34	7.03	8.29	3.77	7.08	4.90	4.79	2.07	17.82

Project 9	I-35 NBL by Hwy. 20
Date	6/11/2003

	Coordinates		Nuc Gage Results			450 mm		300 mm		150 mm	Geogage	
Test #	X	Y	% Moisture	Dry Density, kg/m^3	CIV	Mean DCP Index, mm/blow	Mean Change in DCP Index, mm/blow	Mean DCP Index, mm/blow	Mean Change in DCP Index, mm/blow	Mean DCP Index, mm/blow	Stiffness, MN/m	Modulus, kPa
1	0	-12	9.7	1687	6.7	14.66	3.30	15.92	5.67	18.75	2.51	21.81
2	0	-6	7.0	2079	12.3	29.91	5.70	26.67	3.33	25.00	2.53	47.97
3	0	0	6.9	2074	10.4	26.89	8.33	25.67	8.67	30.00	4.60	39.92
4	0	6	7.9	2034	11.3	25.96	1.06	26.19	0.95	25.71	5.52	47.92
5	0	12	7.5	2030	5.9	36.48	2.13	37.23	4.05	39.25	4.16	36.07
6	4	12	9.2	2042	11.7	34.43	16.61	34.44	22.13	23.38	4.13	35.80
7	4	6	8.3	2064	12.1	30.64	6.30	26.67	1.33	26.00	5.12	44.39
8	4	0	8.5	1970	12.0	38.86	11.25	42.87	20.93	53.33	5.54	48.03
9	4	-6	6.7	2123	11.1	27.10	7.44	26.07	7.86	30.00	5.56	48.26
10	4	-12	12.3	1969	8.2	40.22	18.33	47.33	30.67	62.67	2.84	24.66
11	8	-12	9.8	1752	6.9	60.00	4.00	58.67	8.00	54.67	3.07	26.62
12	8	-6	11.1	1991	13.8	23.11	3.72	23.23	5.21	25.83	5.36	46.48
13	8	0	7.2	2085	7.5	28.39	4.92	28.58	6.17	25.50	4.31	37.40
14	8	6	7.4	2051	15.6	31.86	10.34	29.49	18.53	20.22	5.39	46.42
15	8	12	9.8	2026	6.4	32.90	15.14	39.50	7.00	36.00	4.48	38.84
16	12	12	8.8	2075	7.9	39.68	10.98	39.90	14.20	32.80	4.95	42.97
17	12	6	8.6	2043	13.6	39.08	27.38	42.02	30.62	26.71	4.59	39.78
18	12	0	7.9	2055	15.0	26.56	1.75	27.33	2.33	28.50	5.88	51.00
19	12	-6	6.6	2122	11.6	36.85	5.20	23.57	1.14	23.00	5.12	44.43
20	12	-12	8.4	2019	5.1	43.96	9.56	48.54	3.58	46.75	1.38	11.94
21	16	-12	10.4	1995	11.4	44.02	18.93	40.70	18.60	50.00	4.29	37.25
22	16	-6	6.8	2059	15.5	25.28	8.42	24.00	8.67	28.33	5.78	50.15
23	16	0	8.0	2188	10.5	33.01	9.73	37.95	3.10	36.40	4.72	40.95
24	16	6	7.1	1962	6.7	36.70	4.65	35.55	3.90	37.50	4.06	35.24
25	16	12	8.3	2083	11.5	41.07	12.28	46.00	6.50	42.75	3.38	30.57
26	20	12	12.6	1941	3.7	43.02	5.73	46.63	1.25	47.25	4.47	38.74
27	20	6	8.3	2047	10.2	36.03	16.45	37.25	19.50	27.50	4.44	30.53
28	20	0	8.3	2084	8.3	33.57	19.60	35.25	29.50	50.00	5.00	43.42

29	20	-6	7.1	2120	11.7	25.13	2.30	24.62	4.10	22.57	6.09	52.82
30	20	-12	8.8	2046	10.9	49.17	5.88	48.75	7.00	52.25	3.50	30.40
31	24	-12	10.2	1882	7.1	50.90	22.05	56.35	40.30	76.50	2.25	19.56
32	24	-6	7.0	2057	12.1	27.43	8.96	31.03	4.73	28.67	4.75	41.24
33	24	0	8.5	2053	12.9	24.59	4.31	23.71	4.00	25.71	5.75	49.90
34	24	6	8.4	1979	9.4	36.45	4.95	34.43	7.65	30.60	4.71	40.85
35	24	12	8.7	2023	3.6	50.73	19.40	59.50	8.33	55.33	6.30	54.67
36	28	12	10.3	1997	5.2	40.89	13.04	47.25	14.00	54.25	5.07	43.95
37	28	6	6.5	2044	12.3	38.33	21.00	41.25	22.17	30.17	4.21	36.54
38	28	0	8.7	2054	9.4	29.64	15.12	29.15	19.19	28.75	4.27	37.07
39	28	-6	6.2	2107	10.8	31.50	3.00	30.35	1.70	30.20	5.42	46.98
40	28	-12	7.0	2117	14.1	35.94	12.79	28.91	8.97	24.43	4.27	37.06
41	32	-12	6.7	2010	7.9	48.56	11.33	52.83	19.67	62.67	3.60	31.25
42	32	-6	8.8	2059	8.7	30.48	7.49	35.00	2.80	36.40	5.41	46.96
43	32	0	8.8	2011	9.1	33.04	7.82	33.46	9.58	28.67	4.41	38.29
44	32	6	7.0	2105	16.3	28.51	11.84	28.51	15.78	20.63	5.79	50.21
45	32	12	8.0	2063	3.3	49.83	15.88	43.75	9.00	48.25	5.15	44.71
46	36	12	9.7	1993	3.8	37.81	9.67	43.88	2.25	45.00	5.88	51.05
47	36	6	8.3	2120	20.9	29.39	12.16	28.69	17.63	19.88	5.96	51.68
48	36	0	7.6	2127	11.1	33.96	6.21	31.57	10.47	26.33	5.11	44.32
49	36	-6	7.7	2070	10.1	48.00	29.25	33.50	10.00	38.50	5.62	48.74
50	36	-12	7.8	2094	5.3	39.58	24.88	34.38	22.75	45.75	3.95	34.27
51	40	-12	10.3	2005	5.2	62.50	19.50	62.75	25.50	50.00	5.93	51.48
52	40	-6	7.8	1932	11.6	46.91	11.63	45.03	19.27	35.40	5.71	49.53
53	40	0	8.4	2047	17.5	36.67	8.75	36.25	12.50	30.00	7.25	62.89
54	40	6	7.4	1995	22.1	27.02	4.21	29.75	0.50	30.00	5.05	43.79
55	40	12	8.6	2010	4.1	42.72	19.25	51.17	26.33	64.33	3.74	32.46
56	44	12	13.1	1914	4.9	43.94	12.17	48.42	21.83	59.33	4.55	39.48
57	44	6	6.0	2054	11.6	37.07	21.90	40.00	23.33	28.33	4.72	40.97
58	44	0	7.7	2005	7.8	32.14	10.71	25.08	0.17	25.17	4.12	35.79
59	44	-6	10.1	1938	6.6	25.82	7.36	30.50	1.33	31.17	4.35	37.74
60	44	-12	10.2	1696	4.8	67.83	13.00	76.00	3.00	77.50	2.73	25.00
61	48	-12	8.9	1999	5.9	33.68	24.81	43.70	39.11	63.25	3.57	30.98
62	48	-6	7.7	1970	6.4	35.23	8.28	36.54	8.42	32.33	5.65	48.98
63	48	0	6.6	2020	11.8	47.81	8.79	47.08	13.17	40.50	5.46	47.37
64	48	6	6.6	1955	8.7	32.10	5.25	31.05	9.10	26.50	5.57	48.32
65	48	12	9.1	1950	5.9	56.47	17.63	64.83	20.33	75.00	3.92	34.01
66	52	12	9.8	1980	10.3	40.68	15.98	44.92	12.83	38.50	4.17	36.17
67	52	6	7.7	2014	8.5	32.53	15.33	34.63	16.25	26.50	4.23	36.71
68	52	0	7.1	2041	10.2	35.30	7.25	32.20	10.40	27.00	4.71	40.82
69	52	-6	15.4	1915	11.4	36.11	11.83	35.17	17.67	26.33	6.23	54.01
70	52	-12	14.3	1939	7.9	25.32	17.08	31.73	29.87	46.67	6.90	59.84
71	56	-12	8.8	2053	4.7	43.33	24.33	59.00	3.33	60.67	7.37	63.97
72	56	-6	9.7	2045	7.2	27.58	6.63	30.58	2.83	29.17	5.16	44.81
73	56	0	7.4	1986	9.6	34.22	7.67	38.75	3.50	40.50	5.05	43.85
74	56	6	7.4	2065	7.1	30.11	3.83	32.00	4.00	34.00	4.34	37.61
75	56	12	10.0	1975	5.5	47.25	10.13	50.88	6.25	47.75	4.15	36.00
76	60	12	12.1	1916	5.4	44.00	5.75	47.13	4.25	49.25	2.83	34.54
77	60	6	9.9	1893	4.9	38.34	14.45	46.29	10.08	51.33	4.09	35.45
78	60	0	7.9	1998	13.6	40.40	12.30	38.60	12.80	45.00	5.36	46.47
79	60	-6	9.5	1969	8.1	33.80	5.17	37.15	0.70	37.50	5.37	46.55
80	60	-12	7.7	1986	5.8	72.50	19.00	83.75	8.50	88.00	2.62	22.71
81	64	-12	10.9	1940	5.1	35.17	4.25	37.75	0.50	37.50	3.80	32.93
82	64	-6	8.4	2060	8.4	32.28	10.45	32.13	14.25	25.00	5.34	46.31
83	64	0	8.0	2037	8.6	29.18	6.23	32.70	3.80	34.60	5.28	45.81
84	64	6	10.1	1981	7.6	37.15	3.55	39.13	2.25	40.25	3.69	32.00
85	64	12	10.0	1997	4.6	46.32	22.19	58.33	16.67	66.67	4.08	35.40
		average	8.7	2012.5	9.3	37.3	11.2	38.9	11.3	39.1	4.7	41.0
		Stdev	1.77	83.14	3.82	9.99	6.64	12.07	9.36	15.17	1.11	9.35

Project 10	Lot S1 Before Ash
Date	9/4/2002

	Coordinates		Nuc Gage Results			600 mm		300 mm		Geogage		
Test #	X	Y	% Moisture	Dry Density	CIV	Mean DCP Index, mm/blow	Mean Change in DCP Index, mm/blow	Mean DCP Index, mm/blow	Mean Change in DCP Index, mm/blow	Stiffness	Modulus	CBR
1	0	-8	6.5	2067	13.7	27.09	6.57	22.85	6.92	8.08	70.09	8.78
2	0	0	7.5	2013	22.9	18.24	4.87	14.34	4.28	10.38	90.09	14.79
3	0	8	7.3	1947	18.8	23.23	9.64	21.00	6.85	6.96	60.35	9.65
4	10	-8	9.7	2015	25.0	20.30	5.93	18.71	6.06	10.93	94.86	10.98
5	10	0	7.5	2028	18.1	23.15	6.92	21.46	6.83	7.65	66.36	9.42
6	10	8	8.1	1972	18.8	17.22	2.97	15.37	2.44	10.82	93.96	13.69
7	20	-8	8.2	1975	21.1	21.24	5.77	18.94	4.20	9.23	80.10	10.83
8	20	0	7.9	2001	25.6	20.76	6.08	17.59	5.53	10.38	90.01	11.77
9	20	8	7.2	1944	28.4	20.52	4.93	17.13	4.53	9.70	84.16	12.12
10	30	-8	9.7	1980	22.2	21.93	4.81	15.00	2.39	13.23	114.79	14.07
11	30	0	10.4	1946	19.4	20.24	6.93	20.39	7.06	8.60	74.63	9.97
12	30	8	7.3	1971	21.5	18.05	4.90	14.53	3.76	10.89	94.46	14.58
13	40	-8	8.5	1918	21.6	24.60	4.79	18.56	4.73	10.09	87.51	11.08
14	40	0	9.4	1901	16.3	25.46	7.43	21.86	7.77	8.68	75.29	9.23
15	40	8	7.4	1914	26.4	16.50	5.12	16.21	5.89	9.15	79.42	12.90
16	50	-8	8.2	1870	18.9	20.04	4.96	14.94	3.59	11.70	101.49	14.13
17	50	0	7.2	1846	21.1	18.31	5.57	12.92	3.88	7.78	67.48	16.63
18	50	8	8.0	1970	28.5	17.77	3.06	17.42	2.71	9.47	82.13	11.90
	Average		8.1	1960	21.6	20.81	5.63	17.73	4.97	9.65	83.73	12.0
	Standard Deviation		1.06	56.18	4.04	2.98	1.56	2.94	1.70	1.58	13.73	2.25

Project 11	Lot S1 After Ash
Date	9/4/2002

Test #	Coordinates		Nuc Gage Results		CIV	600 mm		300 mm		Geogage		% Moisture Lab	CBR
	X	Y	% Moist-ure	Dry Density		Mean DCP Index, mm/blow	Mean Change in DCP Index, mm/blow	Mean DCP Index, mm/blow	Mean Change in DCP Index, mm/blow	Stiff-ness	Modulus		
1	0	-8	8.6	1808	20.2	15.30	3.51	10.37	3.20	19.78	171.57	7.1	21.3
2	0	0	10.2	1837	27.0	15.54	2.83	12.04	2.18	16.88	146.43	7.3	18.0
3	0	8	7.7	1812	24.3	15.97	3.59	10.78	2.45	15.45	134.00	6.1	20.4
4	10	-8	8.0	1789	30.4	14.58	2.91	10.38	1.80	16.34	141.74	5.7	21.2
5	10	0	8.6	1784	29.3	13.72	2.03	9.83	1.32	15.14	131.35	5.5	22.6
6	10	8	8.2	1861	18.4	18.80	5.43	13.61	2.85	21.09	182.93	6.4	15.7
7	20	-8	9.5	1792	26.5	14.36	1.59	10.41	1.00	17.83	154.66	7.7	21.2
8	20	0	9.0	1774	28.3	15.78	2.16	10.96	1.02	19.74	171.22	7.0	20.0
9	20	8	7.4	1874	27.6	14.86	3.24	9.91	1.93	15.44	133.92	6.2	22.4
10	30	-8	10.6	1724	25.3	15.89	3.36	12.95	2.62	19.97	155.88	9.9	16.6
11	30	0	9.7	1771	30.5	15.93	3.03	12.45	2.65	13.30	115.41	7.2	17.3
12	30	8	8.3	1910	31.7	17.61	3.48	12.63	2.84	23.15	200.85	7.4	17.1
13	40	-8	9.1	1774	24.0	15.97	3.73	11.24	2.25	13.99	121.38	7.3	19.4
14	40	0	9.4	1719	18.8	15.91	4.32	11.64	2.43	11.49	99.66	8.2	18.7
15	40	8	8.9	1835	26.3	16.62	2.94	12.67	1.87	13.23	114.73	7.8	17.0
16	50	-8	9.5	1760	17.9	17.90	3.59	12.45	1.79	10.52	91.27	8.0	17.3
17	50	0	7.6	1813	19.6	15.68	3.65	11.04	2.95	17.40	150.96	6.7	19.8
18	50	8	8.5	1833	27.8	16.32	2.42	12.05	2.25	12.62	109.45	7.3	18.0
	Average		8.8	1804	25.2	15.93	3.21	11.52	2.19	16.30	140.41	7.2	19.1
	Standard Deviation		0.89	49.50	4.48	1.25	0.88	1.13	0.64	3.50	29.52	1.03	2.10

Project 12	University-Guthrie	
Date	8/28/2003	

Location	$CBR_{CLEGG\ HAMMER}$	E_{DCP} (M Pa)	CBR (Dcp)	IV (clegg)	PR (mm/blow)	Youngs Modulus $_{Geoguage}$ (MPa)	k (cm/sec)	DD	% fines
1	16.9	81.698	11.03	7.40	18.63	71.69	1.66	97.2	0.18
2	129.2	131.917	23.31	22.20	9.55	107.85	1.34	105.3	0.36
3	277.4	224.526	53.52	33.00	4.55	158.93	2.78	102.6	0.22
4	253.5	208.233	47.58	31.50	5.05	121.89	0.19	110.1	0.42
5	250.4	194.446	42.75	31.30	5.56	150.79	1.47	104.4	0.42
6	466.8	225.347	53.83	43.10	4.52	140.21	2.52	96.6	0.10
7	15.7	70.388	8.74	7.10	22.93	105.41	1.00	95.2	0.41
8	116.2	134.059	23.91	21.00	9.33	134.63	0.42	107.3	0.53
9	346.6	215.620	50.24	37.00	4.81	154.45	0.76	100	0.42
10	342.9	216.424	50.53	36.80	4.78	169.9	0.42	107	0.43
11	421.3	216.027	50.39	40.90	4.80	155.76	1.92	100	0.32
12	417.3	227.622	54.68	40.70	4.46	152.56	0.65	104.6	0.16
13	24.5	72.170	9.09	9.10	22.14	80.09	2.10	94.8	0.39
14	184.1	177.685	37.13	26.70	6.30	153.2	1.15	103.2	0.67
15	330.3	215.620	50.24	36.10	4.81	157.89	0.83	108	0.45
16	355.74	196.061	43.30	37.50	5.49	160.42	1.03	107.5	0.28
17	466.75	219.628	51.71	43.10	4.69	143.68	1.83	101.6	0.14
18	462.53	194.542	42.78	42.90	5.55	176.44	7.31	102.6	0.07
19	10.14	51.627	5.38	5.50	35.33	68.06	1.42	88.7	0.36
20	93.14	158.619	31.10	18.70	7.38	146.7	1.11	100	0.35
21	295.68	216.131	50.43	34.10	4.79	130.77	0.43	107	0.28
22	337.50	206.261	46.87	36.50	5.12	149.72	0.58	104.3	0.14
23	295.68	223.024	52.96	34.10	4.59	156.04	1.53	106.9	0.36
24	292.32	197.631	43.85	33.90	5.43	162.17	7.02	104.9	0.20
25	18.17	60.713	6.93	7.70	28.18	77.71	2.24	92.4	0.35
26	158.52	162.392	32.26	24.70	7.14	130.93	3.00	104	0.19
27	305.88	190.494	41.40	34.70	5.72	153.67	2.22	106	0.31
28	302.46	192.992	42.25	34.50	5.61	125.4	0.54	101.6	0.49
29	253.50	202.254	45.46	31.50	5.26	146.88	1.95	107	0.35
30	316.25	224.287	53.43	35.30	4.55	147.06	2.85	101.2	0.33
Average	251.9	176.9	38.6	29.3	8.9	136.4	1.8	102.4	0.3
Stdev	143.6	55.8	16.1	11.7	8.0	29.5	1.7	5.1	0.1